Pettigrew, T.L., Casey, J.F., Miller, D.J., et al., 1999
Proceedings of the Ocean Drilling Program, Initial Reports Volume 179

3. EXPLANATORY NOTES[1]

Shipboard Scientific Party[2]

INTRODUCTION

In this chapter, we have assembled information that will help the reader understand the basis for our preliminary conclusions and also help the interested investigator select samples for further analysis. This information concerns only shipboard operations and analyses described in the site reports in the Leg 179 *Initial Reports* volume of the *Proceedings of the Ocean Drilling Program*. Methods used by various investigators for shore-based analyses of Leg 179 data will be described in the individual scientific contributions published in the *Scientific Results* volume and in publications in various professional journals.

Authorship of Site Chapters

The separate sections of the site chapters were written by the following shipboard scientists (authors are listed in alphabetical order; no seniority is implied):

Leg Summary: Casey, Miller
Operations: Holloway, Miller, Pettigrew
Igneous Petrology and Geochemistry: Casey, Guo, Miller, Shibata, Thy
Metamorphic Petrology: Casey, Miller, Shibata
Structural Geology: Casey
Physical Properties: Miller, Rao
Downhole Measurements: Boissonnas, Einaudi, Hoskins, Myers
Seismic Experiments: Busby, Gerdom, Hoskins, Myers
Appendix: Shipboard Scientific Party

[1]Examples of how to reference the whole or part of this volume.
[2]Shipboard Scientific Party addresses.

Ms 179IR-103

Numbering of Sites, Holes, Cores, and Samples

Drilling sites are numbered consecutively from the first site drilled by the *Glomar Challenger* in 1968. A site refers to one or more holes drilled while the ship was positioned over a single acoustic beacon. Multiple holes are often drilled at a single site by pulling the drill pipe above the seafloor (out of the hole), offsetting the ship some distance from the previous hole (without deploying a new acoustic beacon), and drilling another hole.

For all Ocean Drilling Program (ODP) drill sites, a letter suffix distinguishes each hole drilled at a single site. The first hole at a given site is assigned the suffix A, the second hole is designated with the same site number and assigned suffix B, and so on. Note that this procedure differs slightly from that used by the Deep Sea Drilling Project (Sites 1–624) but prevents ambiguity between site- and hole-number designations. These suffixes are assigned regardless of recovery, as long as penetration takes place. Distinguishing among holes drilled at a site is important because recovered rocks from different holes, particularly when recovery is less than 100%, are likely to represent different intervals in the cored section.

The cored interval is measured in meters below seafloor (mbsf); subbottom depths assigned to individual cores are determined by subtracting the drill-pipe measurement (DPM) water depth (the length of pipe from the rig floor to the seafloor) from the total DPM (from the rig floor to the bottom of the hole; see Fig. F1). Water depths below sea level are determined by subtracting the height of the rig floor above sea level from the DPM water depth. The depth interval assigned to an individual core begins with the depth below the seafloor at which the coring operation began and extends to the depth that the coring operation ended for that core (see Fig. F1). Each coring interval is equal to the length of the joint of drill pipe added for that interval (~9.4–10.0 m). The pipe is measured as it is added to the drill string, and the cored interval is usually recorded as the length of the pipe joint to the nearest 0.1 m. However, coring intervals may be shorter and may not be adjacent if separated by intervals drilled but not cored or washed intervals.

Cores taken from a hole are numbered serially from the top of the hole downward. Core numbers and their associated cored intervals (in mbsf) are usually unique in a given hole; however, this may not be true if an interval must be cored twice because of caving of cuttings or other hole problems. The maximum full recovery for a single core is 9.5 m of rock contained in a core barrel (6.6 cm internal diameter; Fig. F2). Only rotary core barrel bits were used for recovering core during Leg 179.

Cores are pulled from the core barrels in butylate liners, split into ~1.5-m sections, and transferred into split, 1.5-m butylate core liners for curation and storage. The bottoms of oriented pieces (i.e., pieces that clearly could not have rotated about a horizontal axis in the core barrel) are marked with a red wax pencil to preserve orientation during the splitting and labeling process. Contiguous pieces with obvious features allowing realignment are considered to be a single piece. Plastic spacers are used to separate the pieces. Each piece is numbered sequentially from the top of each section, beginning with number 1; reconstructed groups of pieces are lettered consecutively (e.g., 1A, 1B, 1C, etc.; see Fig. F3). Pieces are labeled only on external surfaces, and, if oriented, a way-up arrow is added to the label.

Recovery rates are calculated based on the total length of a core recovered divided by the length of the cored interval (see Fig. F1). As

F1. Terminology for coring operations and core recovery, p. 23.

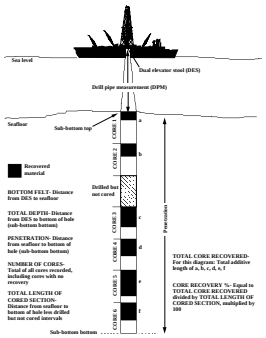

F2. Hard-rock core division procedures, p. 24.

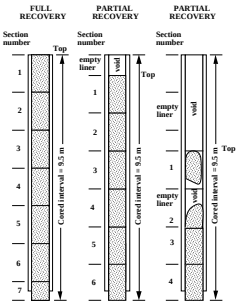

F3. Core curation procedures for hard rocks, p. 25.

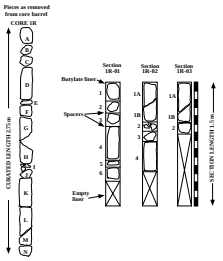

hard-rock coring operations are characterized by <100% recovery, the spacers between pieces can represent intervals of no recovery up to the difference in length between a cored interval and the total core recovered. Most cores are designated "R" (rotary drilled) for curatorial purposes. In instances where coring intervals exceed the 9.5-m length of the core barrel, cores are curated as wash intervals and given the designator "W." Detailed descriptions of each core sampled, thin-section descriptions, and photographs of each core are presented (see the "Core Descriptions" contents list).

Summary Core Descriptions

As an aid to the interested investigator, we have compiled summary information of core descriptions on a section-by-section basis and presented these on hard-rock visual core description (HRVCD) forms (see the "Core Descriptions" contents list). These forms summarize the igneous, metamorphic, and structural character of the core and present graphical representations of the pieces recovered and the lithologic units identified (Fig. F4). The far left side of these forms present an image of the archive half of the core captured shortly after splitting. On the right side of the image, several columns record information about the core. In left-to-right sequence, these columns include archived piece numbers and a graphic representation of piece shape with additional details (veins, fractures, etc.) added to help distinguish features in the image. Next to these is a column indicating pieces that could be oriented relative to way up. The next column indicates the location of shipboard samples. For reference, the samples noted conform to the sampling code in the JANUS database (XRF = X-ray fluorescence analysis; TSB = polished thin section billet; PP = physical properties analysis; and XRD = X-ray diffraction analysis). A graphic lithology column illustrates changes in lithologic units (see "Igneous Petrology and Geochemistry," p. 3); lithologies recovered are represented by the patterns illustrated in Figure F5. A unit number corresponds to each lithologic unit and is recorded in the next column. Metamorphic intensity intervals are represented by uppercase letters (see "Metamorphic Petrology," p. 7). We also present a graphic representation of structural features in the core noting particular structural features (see "Structural Geology," p. 8). On the right side of these forms is a text summary of observations from each section. The upper and lower contacts of each lithologic interval are noted, as well as primary lithology and other comments summarized from igneous descriptions. Text summaries of metamorphic and structural description for each section are also compiled on these forms.

F4. Example of gabbro HRVCD form, p. 26.

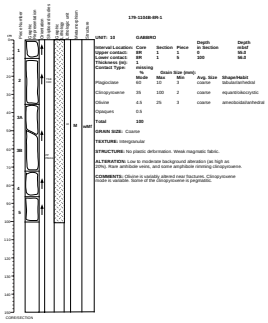

F5. Graphic lithology patterns used during Leg 179, p. 27.

IGNEOUS PETROLOGY AND GEOCHEMISTRY

General Procedures

The procedures for describing igneous rocks during Leg 179, in general, follow the outline presented in the "Explanatory Notes" chapters for Leg 147 (Shipboard Scientific Party, 1993a), Leg 153 (Shipboard Scientific Party, 1995) and Leg 176 (Shipboard Scientific Party, 1999). All igneous petrography and petrology observations are stored in electronic form in project-designed spreadsheets called the igneous-metamorphic core log and are based on the following definitions given below. For a

detailed discussion of core curation and handling, the reader is referred to the "Introduction" section of this chapter. Standard ODP visual core description (VCD) sheets were used to document the igneous rock cores and include both a graphical representation and summaries of the dominant macroscopic features. Descriptions of microscopic features were archived on thin-section description forms. For both the macroscopic and microscopic descriptions, see the "Core Descriptions" contents list.

Igneous intervals were defined on the basis of primary igneous lithologies, textures, and contacts and do not necessarily imply intrusive relationships. The nature of the igneous contacts was systematically recorded together with igneous structures, mineralogy, and textures. Mineral modes and grain sizes were visually estimated and textures and fabric were evaluated based on macroscopic observations. The observations were recorded for each lithologic interval. A summary of the individual measurements is given below.

Rock Classification

The classification of mafic and ultramafic plutonic rocks follows International Union of Geological Sciences (IUGS) recommendations (Le Maitre, 1989; Fig. F6) with minor modifications. We use the term oxide gabbro if the mode exceeds 5% oxide minerals and the modifier oxide-bearing if oxide minerals are present in abundances <5%. The modifier troctolitic was used to describe olivine gabbro when pyroxene represents 5% to 15% of the ferromagnesian assemblage. Lithologies with high proportions (>65%) of mafic minerals were noted as melanocratic, and those with high proportions (>65%) of plagioclase were noted as leucocratic. The modifier micro- was used to distinguish gabbroic rocks with a dominant grain size <1 mm (e.g., microgabbro, microtroctolite, and microgabbronorite). The modifier pegmatitic was used when the average grain size of an interval exceeds 30 mm. Leucocratic rocks with >20% quartz and <1% K-feldspar (a restricted part of the tonalite field of the IUGS classification) were called trondhjemites in keeping with previous usage in the ocean-crust literature.

If a mafic plutonic rock exhibits the effects of dynamic metamorphism such that the assemblage consists of secondary hydrous minerals that completely obliterate the protolith mineralogy and texture, or if the rock is made up of recrystallized primary minerals such that the original igneous protolith cannot be recognized, the appropriate metamorphic rock names were used. The textural terms mylonitic, schistose, and gneissic were added to metamorphic rock names, such as greenstone, amphibolite, or metagabbro, to indicate that the rocks exhibit the effects of dynamic metamorphism.

F6. Classifications of ultramafic, gabbroic, and silicic plutonic rocks, p. 28.

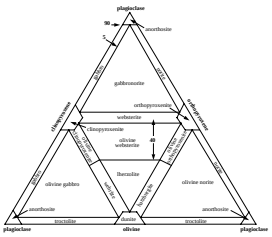

Primary Minerals

The principal rock-forming minerals in the cores are plagioclase, olivine, clinopyroxene, orthopyroxene, Fe-Ti oxides, and sulfides. For each of these minerals, the following data were recorded on the VCDs and in electronic form on spreadsheets (igneous lithology and contacts log; see Fig. F7):

1. Estimated modal percent of the primary minerals;
2. Smallest and largest size of mineral grains (measured along the longest axis in millimeters);

F7. Example of igneous/metamorphic core-description spreadsheets, p. 31.

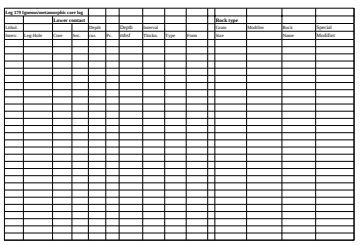

3. Average crystal size for each mineral phase; and
4. Percentage of primary minerals replaced by secondary phases.

From these data, a lithology name based on IUGS definitions was generated by a "Visual Basic for Applications" macro in the spreadsheet. An overall grain size was assigned using the terms fine grained (<1 mm), medium grained (1–5 mm), coarse grained (5–30 mm), and pegmatitic (>30 mm). Also recorded were descriptions of mineral shapes using terms such as equidimensional, tabular, prismatic, platy, elongate, acicular, skeletal, and amoeboidal, and descriptions of mineral habit using the terms like euhedral, subhedral, anhedral, rounded, deformed, and fractured.

Igneous Textures

Textures of the plutonic rocks were characterized on the basis of grain shape, mutual contacts, and preferred mineral orientation. Rock textures such as equigranular, inequigranular, intergranular, and granular were used to describe the overall texture of each lithologic interval. Poikilitic, ophitic, subophitic, and interstitial textures were distinguished according to the predominant grain shapes in each interval. No attempt was made to apply classic cumulus terminology (Wager et al., 1960) during macroscopic rock descriptions, but these terms were used in the thin-section descriptions where appropriate (see **"Thin-Section Description,"** p. 6). Igneous fabrics that were distinguished include lamination and lineation. These terms were reserved for rocks exhibiting a clear preferred dimensional orientation of mineral grains that was likely derived from magmatic processes.

Igneous Structures

In plutonic rocks, igneous structures can be especially important in defining the mechanism of crystallization of the primary mineralogy (Irvine, 1982). Igneous structures noted in the core description include layering or lamination, igneous contacts, gradational grain-size variations, gradational modal variations, gradational textural variations, and breccias. Layering was used to describe vertical changes in grain size, mode, or texture within an interval. Grain-size variations were described as normally graded if the coarser fraction is at the bottom and reversely graded if the coarser fraction is at the top. Modal variations were described as normal if mafic minerals are more abundant at the bottom and reversed if mafic minerals are more abundant at the top. Igneous breccia was noted if the breccia matrix appears to be of magmatic origin.

Contacts between Lithologic Intervals

The nature of igneous and lithologic contacts is an important observation as it provides clues to the origin of the downhole lithologic and structural variation in the core. Attempts were made to distinguish internal layer contacts within a single pluton, igneous intrusive contacts between plutons, and/or structural contacts between intervals. The most common types of contacts observed were those without chilled margins. These were described as planar, curved, irregular, interpenetrative, sutured, or gradational. In many cases, contacts were obscured by subsolidus or subrigidus deformation and metamorphism

and were called sheared if an interval with deformation fabric is in contact with an undeformed interval, foliated if both intervals have deformation fabrics, or tectonic if the contact appears to be the result of faulting or localized ductile shearing.

Thin-Section Description

Thin sections of igneous rocks were examined to complement and refine the hand-specimen observations. In general, the same types of data were collected from thin sections as from hand-specimen descriptions. Cumulate terminology (Wager et al., 1960) was applied where appropriate. Modal data were collected using standard point-counting techniques or visual estimation. All data are summarized in ODP format thin-section descriptions (see the **"Core Descriptions"** contents list). Crystal sizes were measured using a micrometer scale and are generally more precise than hand-specimen estimates. The presence of inclusions, overgrowths, and zonation was noted, and the apparent order of crystallization was suggested in the comment section for samples with appropriate textural relationships. The presence and relative abundance of accessory minerals such as Fe-Ti oxides, sulfides, apatite, and zircon were noted. The percentage of alteration was also reported (see **"Metamorphic Petrology,"** p. 7).

Igneous Lithology, Interval Definitions, and Summary

For a complex sequence of plutonic rocks, interpretations of the lithologic successions in the core are difficult because of overprinting of synmagmatic, metamorphic, and tectonic processes. The lithologic intervals adopted here are defined by vertical sections with consistent internal characteristics and lithology and are separated based on geological contacts defined by significant changes in modal mineralogy, grain size, or primary texture, as encountered downhole. To the extent possible, boundaries were not defined where changes in rock appearance were only the result of changes in the type or degree of metamorphism or the intensity of deformation. Both sharp and gradational contacts occur between intervals. If the contact was recovered, its location is recorded by the core, section, position (in centimeters), and piece number. If the contact was not recovered, but a significant change in lithology or texture was observed, the contact was placed at the lowest piece of the upper interval. The information recorded for each section of the core includes the rock type; igneous, metamorphic, and/or deformational texture; evidence for igneous layering; extent, type, and intensity of deformation; primary and secondary minerals present; grain shape for each primary mineral phase; evidence of preferred orientation; the position of quartzo-feldspathic veins (whether of igneous or hydrothermal origin); and general comments. The description and summary of each interval was entered on the standard ODP form where the general lithological description and top and bottom of the interval are recorded with reference to curated core, section, piece(s), depth, and thickness.

Geochemistry

Samples considered by the Shipboard Scientific Party to be representative of the various lithologies cored were analyzed for major oxide and selected trace element compositions with the shipboard ARL 8420

wavelength-dispersive XRF apparatus. Full details of the shipboard analytical facilities and methods are presented in previous ODP *Initial Reports* volumes (e.g., Leg 118, Shipboard Scientific Party, 1993a; Leg 140, Shipboard Scientific Party, 1992b; Leg 147, Shipboard Scientific Party, 1993a; Leg 153, Shipboard Scientific Party, 1995). A list of the elements analyzed and the operating conditions for Leg 179 XRF analyses are presented in Table T1.

T1. XRF analytical conditions for Leg 179, p. 45.

After coarse crushing, samples were ground in a tungsten carbide shatterbox. Then, 600-mg aliquots of ignited rock powder were intimately mixed with a fusion flux consisting of 80 wt% lithiumtetraborate and 20 wt% heavy absorber La_2O_3. The glass disks for the analysis of the major oxides were prepared by melting the mixture in a platinum mold in an electric induction furnace. Trace elements were determined on pressed powder pellets prepared from 5 g of rock powder (dried at 110°C) mixed with a small amount of a polyvinyl alcohol binder solution. The calibration of the XRF system was based on the measurement of a set of reference rock powders. A Compton scattering technique was used for matrix absorption correction for trace element analysis. Loss on ignition for each sample was determined by the standard practice of heating an oven-dried (110°C) 20-mg sample to 1010°C for several hours.

METAMORPHIC PETROLOGY

The procedures and methods for metamorphic descriptions of the core during Leg 179 generally follow those adopted during Leg 147 (Shipboard Scientific Party, 1993a), Leg 153 (Shipboard Scientific Party, et al., 1995), and Leg 176 (Shipboard Scientific Party, 1999). VCDs of metamorphic characteristics were compiled together with igneous and structural documentation of the core. This information was recorded to provide two types of information: (1) the extent of replacement of igneous minerals by metamorphic or secondary minerals and (2) the extent to which metamorphic or alteration minerals contribute to any subsolidus fabric found in the core. These data were recorded together with igneous descriptions in the igneous/metamorphic core log (see Table AT2.XLS in the "Appendix" contents list) and are summarized in the VCDs. To ensure accurate core descriptions, thin-section petrography of representative samples was integrated into the VCDs. Identification of mineral phases was, when possible, confirmed by XRD analyses according to ODP standard procedures outlined in previous *Initial Reports* volumes (e.g., Volume 118; Shipboard Scientific Party, 1989a). Terminologies adopted for metamorphic rock types, metamorphic textures and fabrics, metamorphic facies, etc., follow conventional usage (Williams et al., 1982). Metamorphic mineral assemblages and alteration intensities are included in the comments column of the igneous/metamorphic core log (see Table AT2.XLS in the "Appendix" contents list). Alteration intensity was classified as negligible (<2%), slight (2%–10%), moderate (10%–40%), high (40%–80%), and pervasive (80%–100%). Portions of pieces where primary textures were ambiguous or obliterated by secondary minerals were termed patches. For those patches where thin-section analysis was available, their mineralogies are recorded (see the "Core Descriptions" contents list).

Description of Metamorphic Fabrics

Where metamorphic minerals are included in fabric elements such as shear zones, cataclastic fabrics, foliations, textures and associated minerals were recorded in the structure log (see Table AT3.XLS in the "Appendix" contents list). For samples affected by crystal-plastic deformation, textural features noted included identities and abundances (in volume percent) of porphyroclasts and their alteration products, neoblasts, and other minerals associated with and defining the fabric.

Breccias were defined as intervals of angular fragments in which clast rotation could be documented. Portions of the core crosscut by dense vein networks may appear to be brecciated; however, if adjacent clasts separated by the veins were not visibly rotated, they were described as net or mesh veined. Characterization of breccias included clast lithology and secondary phase mineralogy, matrix mineralogy, and abundances of clasts and mineral phases.

Thin-Section Description

Detailed petrographic descriptions were made aboard ship to aid in identification and characterization of metamorphic and vein mineral assemblages. Stable mineral parageneses were noted, as were textural features of minerals indicating overprinting events (e.g., coronas, overgrowths, and pseudomorphs). Mineral abundances were visually estimated. These data are recorded and summarized (see the "Core Descriptions" contents list). The modal data allowed accurate characterization of the intensity of metamorphism and aided in establishing the accuracy of the macroscopic visual estimates of the extent of alteration.

STRUCTURAL GEOLOGY

Conventions for structural studies established during previous hard-rock drilling legs (e.g., Leg 118, Shipboard Scientific Party, 1989a; Leg 131, Shipboard Scientific Party, 1991; Leg 135, Shipboard Scientific Party, 1992a; Leg 140, Shipboard Scientific Party, 1992b; Leg 141, Shipboard Scientific Party, 1992c; Leg 147, Shipboard Scientific Party, 1993a; Leg 148, Shipboard Scientific Party, 1993b; Leg 153, Shipboard Scientific Party, 1995; Leg 176, Shipboard Scientific Party, 1999) were generally followed during Leg 179. However, several minor changes in nomenclature and procedure were adopted. These changes are described below. Where procedures followed directly from previous legs, references to the appropriate "Explanatory Notes" chapters are given. Leg 179 was originally designed as an engineering leg, but because of contingencies that developed before and during the cruise that required core recovery, the leg was significantly understaffed, based on the core recovered. Description efforts were concentrated, therefore, on completing structural information for the VCDs (Fig. F4). VCD information was entered as basic log sketches with positions of measurements on the core. In addition, preliminary descriptions of each core section were made and recorded in structural notebooks, and the information was later transcribed into a word-processing program and summarized for the VCD form. The positions of as many major structural features as possible were also logged, and many of these features were oriented on the core face. These data were entered into the

structural log spreadsheet (Fig. F8). More detailed structural measurements and descriptions of the core and thin sections will await shore-based studies.

Overview of Macroscopic Core Description

Following procedures described in the Leg 153 Initial Reports volume (Shipboard Scientific Party, 1995), data were entered onto a VCD form (Fig. F4). The structural sketches drawn onto the VCD were designed to present the most representative structures and crosscutting relationships present on a core, in conjunction with the brief general descriptions printed on the same form. Where no structures or fabrics were present, the structural column was left blank. Six spreadsheet logs used during previous legs (see Cannat, Karson, Miller, et al., 1995; Dick, Natland, Miller et al., 1998) were combined into a single structure log spreadsheet (Fig. F8) for identifying the positions and describing major structural features, fabric zones, or structural unit boundaries.

Paper copies of the spreadsheet form were used for recording specific structures and measurements during core description. The structural log spreadsheet was used to record data on joints, veins, foliations, folds, fault and magmatic breccias, faults and fault zones, cataclastic, mylonitic and gneissic shear zones, crystal-plastic fabrics, sense of shear indicators, magmatic fabrics, mineral lineations, slickenlines, compositional layering, igneous plutonic contacts, and crosscutting relationships. Each feature and structural zone has been logged into the structure log with its position. Limited orientation data were gathered because of the lack of sufficient time given the small number of scientific personnel assigned to the leg. The description and orientation of structural features were recorded using curated depth so that "structural intervals" can easily be correlated with other lithologic intervals. Descriptions and structural measurements were based on observations on the working half of the core (see "Structural Measurements," p. 9).

Nomenclature

Structural Identifiers

To maintain consistency of core descriptions of plutonic rocks during previous legs, we used feature "identifiers" for structures similar to those outlined during Leg 153 (Shipboard Scientific Party, 1995) and Leg 176, (Shipboard Scientific Party, 1999) although some modifications should be noted in Figure F9. The characteristics of each structure in the identifier list that were investigated are listed in Figure F10. For major structural features, a planar and/or linear orientation, usually limited to a single apparent dip (or plunge) on the core face, was recorded, and the comments section in the structural log (Fig. F8) was used for additional explanatory remarks.

Structural Measurements

Structural features were recorded relative to core section depths in centimeters from the top of the core section. Depth was defined as the point where the structure intersects the center of the cut face of the working half of the core, as detailed in the Leg 153 *Initial Reports* "Explanatory Notes" chapter (see fig. 15A in Shipboard Scientific Party,

F8. Example of structural log spreadsheet, p. 37.

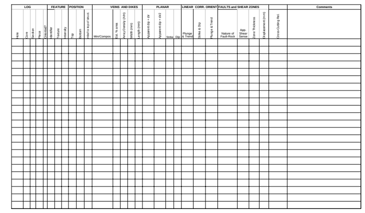

F9. Key to structural identifiers used during Leg 179, p. 38.

	Leg 179 Structural Identifiers	
Identifiers	Planar Feature	Linear Feature
J	Joints	
SHM	Drilling Induced Sub-horizontal Microcracks	
AV	Alteration Veins	Mineral Growth Direction
MV	Magmatic Veins	Mineral Growth Direction
DC	Igneous Dike Contact	Mineral Lineation
IPC	Igneous Pluton Contact	
F	Faults	Slickenlines
B	Fault Breccias	Slickenlines
MB	Magmatic Breccias	
CB	Cataclastic Breccias	
BFZ	Brittle Fault Zone	Slickenlines
CSZ	Cataclastic Shear Zone	
MSZ	Mylonitic Shear Zone	Mineral Lineation
DSZ	Ductile Gneissic Shear Zone	Mineral Lineation
AF	Anastomosing Foliation	Mineral Lineation
DF	Disjunctive Foliations	Mineral Lineation
CPF	Crystal-Plastic Shape Fabric	Mineral Lineation
FO	Folds	Fold Hinge
MF	Magmatic Fabric	Mineral Lineatiom
ILC	Igneous Layer Contact	
ILZ	Zone of Fine Scale Igneous Layering	
TI	Boundary Between Tectonite and Igneous Textured Rock	
B	Bedding	
UNC	Unconformities	
VFB	Volcanic Flow Boundaries	

F10. Table showing checklist used for spreadsheet comments associated with each structural identifier, p. 39.

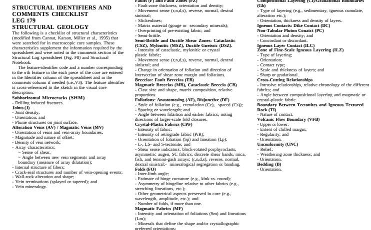

1995). Crosscutting relationships were described in intervals delimited by top and bottom depth.

Apparent fault displacements were recorded as they appeared on the cut face of the archive half of the core and the end of broken pieces. Displacements seen on the core face were treated as components of dip-slip movement, either normal or reverse. Displacements of features visible on the upper and lower surfaces of core pieces were treated as components of strike-slip and termed sinistral or dextral. Displacements were measured between displaced planar markers, parallel to the trace of the fault. Additional cuts and slickenside orientations were incorporated wherever possible to differentiate between apparent dip-slip, oblique-slip, and strike-slip displacements.

The measurement of the orientations of observed structures was oriented with respect to the core reference frame (working half). The convention we used for the core reference frame is the same as detailed in Shipboard Scientific Party (1995) and shown at the top of the comments box in the structural data spreadsheets (see the **"Appendix"** contents list). All spreadsheet orientations are given in the core reference frame.

Planar structures were oriented using the techniques outlined during Legs 131 (Shipboard Scientific Party, 1991) and 153 (Shipboard Scientific Party, 1995). Apparent dip angles of planar features were measured on the cut face of the working half of the core. To obtain a true dip value, a second apparent dip reading will be obtained where possible during postcruise investigations in a section perpendicular to the core face (second apparent orientation). Apparent dips in the cut plane of the working core were recorded as a two-digit number (between 00° and 90°) with a dip direction to 090° or 270°. In the second plane, apparent dip directions will be recorded as either 000° or 180°. The dip and the dip direction for the working half of the core were recorded on the spreadsheet together with second plane measurements. If the feature intersected the upper or lower surface of the core piece, measurements were made directly of the strike and dip in the core reference frame. Where broken surfaces exposed lineations or striations, the trend and plunge were measured directly, relative to the core reference frame. All structural measurements for each feature were entered into the structural log spreadsheet (Fig. **F8**).

The second stage of core orientation, involving a combination of two apparent dips to calculate a true dip and rotating the azimuthal data to fit with the paleomagnetic data, was not completed on board because no paleomagnetist sailed during Leg 179. In this step, adding or subtracting, as appropriate, the difference between the 000° reference direction and magnetic north, the core measurements can be rotated into a geographically correct orientation. This procedure is outlined in steps in figure 6 of Shipboard Scientific Party (1991). Detailed measurements will be completed onshore.

Fabric Intensities and Textural Terms

A key for fabric intensity (Fig. **F11**) and a list of textural abbreviations (Fig. **F12**) were used to refine identifier descriptions. When feasible, quantitative and semi-quantitative estimates of feature development were used to define a five-category relative intensity scale. It is important to recognize that this scale is based on different characteristics for different types of structures and that not all of the identifiers could be appropriately assigned an intensity value. We also emphasize that the

F11. Table showing intensity scales applied to structural identifiers for brittle and ductile deformation, **p. 40.**

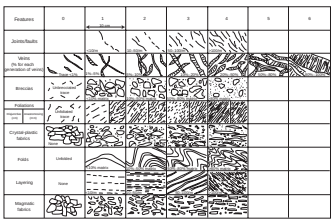

F12. Key to textural features entered in structural VCDs and summary spreadsheet, **p. 41.**

Textures	Code	Abreviation
Protogranular	1	PG
CG Equigranular	2	CGE
Porphyroclastic	3	PC
Elongate Porphyroclastic	4	EPC
Mylonitic	5	MYL
UltraMylonitic	6	UMYL
Cataclastic	7	CAT
Equigranular Gneiss	8	EG
Augen Gneiss	9	AG
Schistose	10	SCH

intensity estimates were only semiquantitative at best and could not be fully quantified during core description. Frequent cross-checks were used between shipboard structural geologists to ensure consistency during core description. The intensity scales are represented in Figure F11 and summarized below:

1. For joints and faults, the intensity scale relates to spacing (i.e., density) estimated by the linear intercept method along the central divide of the core piece. If a piece was unoriented, then spacing was estimated along the long axis of the piece. As no stereological corrections were applied, these values remain at best semiquantitative.
2. Vein intensity is related to an estimation of percentage of veining on the cut face of the archive half of the core. In contrast to other intensity scales, the vein scale has been subdivided into seven groups so the relatively low percentages encountered during Leg 179 could be distinguished. The densities of vein arrays were also recorded separately on the spreadsheet.
3. Brecciation intensity relates to the relative percentage of clasts to matrix.
4. Foliation intensities broadly relate to the spacing of foliation planes. In the case of an anastomosing foliation, the closer the foliation planes and the more planar they become, the higher the intensity value.
5. Crystal-plastic fabric intensities relate to the attenuation and degree of preferred alignment of porphyroclasts and the degree of preferred alignment of any mineral grains.
6. Fold intensity relates to the interlimb angle for individual or multiple folds.
7. Layering intensity relates only to the layer width and was applied to any repeated layers with discrete or gradational boundaries. Such layers included primary magmatic layering, alteration, or grain-size variations.
8. Magmatic deformation intensity relates broadly to the degree of shape preferred orientation of magmatic phases.

Nine textural classes were selected for the purpose of macroscopic description (Fig. F12). It must be stressed that these classes do not necessarily directly relate to any single physical parameter such as stress or strain. Moreover, some of these terms apply only to mafic rocks, others to ultramafic rocks, and some to both of them. The primary reason for selecting these classes was that they are relatively unambiguous textural terms. The definitions below were designed primarily for hand-sample observations where thin sections were not necessarily available. Coarse-grained equigranular refers to a rock that has been deformed but shows no marked grain-size reduction. Porphyroclastic refers to a polymodal grain-size distribution; medium-grained (1–5 mm) elongated porphyroclasts are embedded in a relatively fine-grained (typically <<1 mm) matrix. Gneissic refers to compositional banding in a ductilely deformed rock, where porphyroclasts are commonly elongated parallel to the banding. Schistose refers to the visibility of platy or prismatic metamorphic minerals that define a preferred dimensional orientation and typically a parallel fissility. Magmatic was used for those rocks displaying a well-developed shape-preferred orientation, but where the magmatic character of the individual crystals has not been destroyed by solid-state deformation. The terms mylonitic, ultra-mylonitic, and cataclastic were

used in accordance with the definitions presented by Twiss and Moores (1992).

Thin-Section Descriptions

Thin sections were examined to characterize the microstructural aspects of important mesoscopic structures in the core. Classes of information that were obtained include deformation mechanisms on a mineral-by-mineral basis, kinematic indicators, crystallographic and shape fabrics, qualitative estimates of the degree of crystallographic preferred orientation along local principal finite strain axes, syn- and postkinematic alteration, and the relative timing of microstructures.

Thin sections were oriented, where possible, with respect to the core axis and in the core reference frame described in "**Structural Measurements**," p. 9. Selected samples were cut perpendicular to the foliation and parallel to any lineation to examine kinematic indicators and the shape-preferred orientation of minerals (See fig. 15 of Shipboard Scientific Party, 1995). We adopted and modified the thin-section description form used by the structural geologists during Leg 140 (Shipboard Scientific Party, 1992b) and 153 (Shipboard Scientific Party, 1995), and microstructural information is reported in the thin-section report.

The terms used to describe microstructures generally follow those used during Leg 153 and Leg 176. It is possible that superposition of different microstructures or deformation mechanisms may occur during solidification and subsolidus cooling. Thus, the physical state of the material during fabric development may span the transition from magmatic to solid state. Fabrics defined entirely by igneous minerals with no crystal-plastic deformation microstructures, we term magmatic. Where local crystal-plastic fabrics are associated with melt-enhanced diffusion-related mechanisms including (1) melt-enhanced diffusion creep (Hirth and Kohlstedt, 1995), (2) submagmatic microfracturing (Bouchez et al., 1992), and/or (3) contact melting or pressure solution (Means and Park, 1994; Nicolas and Ildefonse, 1996), we term the physical state crystal-plastic ± melt. Where fabric development is accommodated entirely by dislocation climb/creep, we use the term crystal-plastic to define the physical state of the rock. The other groups refer to rocks with magmatic and/or crystal-plastic texture overprinted by brittle deformation.

PHYSICAL PROPERTIES

Laboratory measurements of the physical properties of igneous and metamorphic rocks are used to indicate major lithologic changes, to help identify intervals of high magnetic susceptibility, to recognize changes in paleomagnetic character, and to allow preliminary interpretation of seismic velocity profiles. During Leg 179, when only gabbroic rocks were sampled, measurements were made of magnetic susceptibility, rock magnetism, bulk density (wet and dry), porosity, compressional wave (*P*-wave) velocity, and natural gamma-ray emission. We made measurements on whole core sections (magnetic susceptibility and gamma ray emission), split core (remanent magnetization), and on discrete minicore samples (*P*-wave velocity at ambient pressure and index properties).

Whole-Core Multisensor Track Measurements

The multisensor track (MST) is an automated and rapid core-conveying and positioning system with multiple in-line sensors/detectors that allow a user-defined series of measurements. At preselected sampling intervals, this system provides a display of measured values and allows rapid data archiving in the ODP database for evaluation of these properties with depth. Inasmuch as the *P*-wave velocity and gamma-ray attenuation porosity evaluator devices were designed for optimum performance when core liners are completely full (as is common in sediment coring, but which never occurs with hard-rock recovery), these measurements were not made during Leg 179. Additionally, although we expected little response above baseline values for natural gamma emission from the lithologies recovered, these measurements were intermittently made as a systems check. During Leg 179, we routinely sampled magnetic susceptibility at a constant 4-cm interval to optimize time and minimize the potential of missing thin intervals of oxide-bearing lithologies.

Magnetic Susceptibility

Magnetic susceptibility (k) is the ease or degree to which a material is magnetized in an external field and is a measure of the concentration of ferromagnetic grains. The Bartington MS2C susceptometer loop on the ODP MST has a measurement range of 1×10^{-5} to 9999×10^{-5} (SI, volume specific) or 1×10^{-8} to 9999×10^{-8} (SI, mass specific). This sensor operates at a frequency of 0.565 KHz and an alternating field intensity of 80 A/m. Temperature drift effects are less than 10^{-5} SI/hr and the resolution of the loop sensor is 2×10^{-6} SI at 9-s measurement intervals.

Natural Gamma Radiation

Gamma rays are spontaneously emitted by the atomic nuclei of elements during natural radioactive decay. In rocks, the elements of interest are most commonly potassium (half-life = 1.3×10^9 years), thorium (half-life = 1.4×10^{10} years), and uranium (half-life = 4.4×10^9 years). The emission of natural gamma radiation is routinely measured on ODP cruises in electron volts (eV) or GAPI (gamma-ray, American Petroleum Industry) units for correlation with downhole logging measurements. Details of the measurement system are available in ODP Technical Note 26 (Blum, 1997). Natural gamma radiation measurements were made for calibration and system-check purposes only during Leg 179.

Split-Core Magnetic Measurements

Archive halves of the split core were processed in the 2-G Enterprises pass-through magnetometer. With this instrument, sensors measured intensity and direction of natural remanent magnetization at stepped demagnetization intervals to 20 mT.

Discrete Sample Measurements

One-inch diameter minicore samples were extracted from the working half of the core on a routine basis for measurements of physical properties. Measurement techniques for index properties (bulk density,

grain density, water content, porosity, and dry density) are documented in ODP Technical Note 26 (Blum, 1997), and specific techniques for hard-rock measurements were applied as described in Shipboard Scientific Party (1999).

P-wave velocity at ambient pressure was determined by the pulse transmission method utilizing piezoelectric transducers as sources and detectors in a screw-press modified Hamilton Frame, as described by Boyce (1976). All measurements were made on seawater-saturated minicores cut perpendicular to the axis of the core (diameter = 2.54 cm; approximate length = 2 cm) at zero confining pressure.

Minicores used for the *P*-wave velocity measurements were resaturated with seawater in a vacuum for 24 hr before measurement. Flat ends of the minicores were carefully smoothed with 240 carbide grit on a glass plate to ensure parallel faces. The length of each minicore was checked using a caliper along its circumference, and grinding continued until all length measurements were within 0.02 mm. Before measurement, the grit was removed by thoroughly cleaning the samples in an ultrasonic bath. Distilled water was used to improve the acoustic contact between the sample and the transducers.

Calibration measurements were performed during the cruise using polycarbonate standard minicores of varying lengths in order to determine the zero-displacement time delay inherent in the measuring system. Results were output in meters per second.

DOWNHOLE MEASUREMENTS

Introduction

Downhole logs are used to directly determine the physical, chemical, and structural properties of formations penetrated by drilling. Where core recovery is incomplete, logging data may serve as a proxy for physical properties and sedimentological and petrological data. These data complement the discrete measurements obtained from cores and offer advantages over core-based analyses in that they are collected rapidly and represent continuous, in situ measurements of the formation. Logs also provide a link between core and the seismic measurements. Sonic velocity logs improve traveltime-to-depth conversion. During Leg 179, four standard logging strings were deployed at Site 1105.

Logging Tool Strings

Logging tools are joined together in tool strings (Fig. **F13**) and are run sequentially into the hole on a seven-conductor cable. Tool strings deployed during Leg 179 included the dual induction/array sonic/gamma ray/temperature tool string, Formation MicroScanner/gamma ray tool string, density/porosity/gamma tool string, and the borehole compensated sonic/gamma tool string (Fig. **F13**). Every Schlumberger tool and tool measurement used during Leg 179 has an associated three- or four-letter acronym. These are shown in Table **T2**. Specifications for each tool are presented in Table **T3**.

Principles and Uses of the Tools

The principles of operation and uses of the tools are described in detail in Serra (1984, 1986), Timur and Toksöz (1985), Ellis (1987), Rider

F13. Downhole logging tool strings used for Leg 179, **p. 42.**

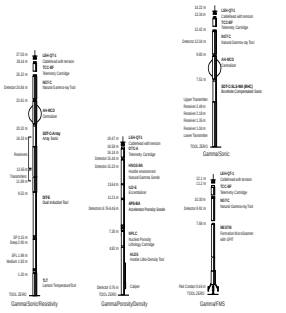

T2. Schlumberger tool and measurement acronyms, **p. 46.**

T3. Specifications of the downhole tools deployed during Leg 179, **p. 47.**

(1996), in the "Explanatory Notes" chapter of the Leg 176 *Initial Reports* volume (Shipboard Scientific Party, 1999), and briefly below.

Dual Induction/Array Sonic/Gamma/Temperature Tool String

The dual induction tool (DIT) provides three different measurements of electrical resistivity, each of which penetrates the formation to a different depth and has a different vertical resolution (Table T2; Fig. F13). Values are recorded every 0.1524 m. Water content and salinity are the most significant factors controlling the resistivity of rocks. Resistivity is therefore primarily related to the inverse square root of porosity (Archie, 1942). The other main factors influencing the resistivity of a formation include the concentration of hydrous and metallic minerals, hydrocarbons and gas hydrates, and the abundance, distribution, and geometry (tortuosity) of interconnected pore spaces. The DIT is a valuable tool in defining lithologic boundaries.

The array sonic digital tool (SDT) is aimed at maximizing the information obtained from measured sonic waveforms by acquiring a digitized full-sonic waveform downhole. This is achieved by using two transmitters and receivers with a 1-m spacing in addition to a linear array of eight receivers spaced at 15 cm (Fig. F13). The addition of a linear array in place of two discrete receivers is the main change in the SDT from earlier tools. The digitally recorded full-wave form is used postcruise to determine shear-wave (*S*-wave) and Stoneley wave velocities in addition to the real time compressional wave (*P*-wave) velocity. Standard vertical resolution is 60 cm, although special array processing can produce a 15-cm resolution.

The natural-gamma spectrometry tool (NGT) measures the natural radioactivity of the formation using a NaI scintillation crystal mounted inside the tool. In formations, gamma rays are emitted by the radioactive isotope ^{40}K and by the radioactive isotopes of the U and Th decay series. Measurements are analyzed by dividing the incident gamma-ray signature into five discrete energy windows, which correspond to the main spectral peaks for each element. The total counts recorded in each window, for a specified depth in the well, are inverted to give the elemental abundances of K (wt%), U (ppm), and Th (ppm). The NGT also provides a measure of the total gamma-ray signature (SGR or K + U + Th) and a uranium-free measurement (CGR or Th + K). Values are recorded every 0.1524 m, and the vertical resolution of the NGT is on the order of 46 cm (Table T2). The natural gamma-ray measurement is commonly used to estimate the clay or shale content because there is a relatively high abundance of radioactive elements in clay minerals. There are rock matrices, however, for which the radioactivity ranges from moderate to extremely high values because of the presence of volcanic ash, potassic feldspar, or other radioactive minerals.

The Lamont-Doherty Earth Observatory (LDEO) temperature-logging tool (TLT) is a self-contained, high-precision, low-temperature tool for recording borehole temperature. Because drilling and circulation operations disturb the temperature conditions in the borehole, the data recorded by the TLT are unlikely to match equilibrated formation temperatures. Nevertheless, the spatial temperature gradient is useful in identifying abrupt gradient changes that commonly indicate localized fluid seepages from the formation.

FMS/Gamma

The Formation MicroScanner (FMS) produces high-resolution images of the resistivity of the borehole wall. The tool has four orthogonally oriented pads, each having 16-button electrodes that are pressed against the borehole wall (Serra, 1989). The tool works by emitting current from the four pads into the formation. The current intensity variations are measured by an array of receptors on each of the four pads. Roughly 30% of a 25-cm diameter borehole is imaged. The vertical resolution is ~5 mm, allowing features such as clasts, thin beds, fractures, and veins to be imaged. The images are oriented so that both strike and dip can be obtained for the formation fabric.

Porosity/Density/Gamma

The hostile-environment natural gamma-ray sonde (HNGS) measures the natural gamma radiations from isotopes of K, Th, and U in the formation surrounding the tool. As opposed to the NGT, the HNGS uses larger bismuth germanate crystals, which detect a higher number of emitted photons. High K and Th values indicate greater clay concentrations.

The accelerator porosity sonde (APS) emits fast neutrons, which are slowed by hydrogen in the formation, and the energy of the rebounded neutrons is measured at detectors spaced along the tool. Abundant hydrogen is in the pore water, hence porosity may be derived. However, hydrogen bound in minerals such as clays also contributes to the measurement. As a consequence, the true porosity value is often overestimated. The neutrons slowed to thermal energies are captured by nuclei, especially those of chlorine and the heavier elements; this effect is measured by the APS as the neutron capture cross section.

The litho-density sonde (HLDS) emits high-energy gamma rays, which are scattered by the electrons in the formation. The electron density, and hence the bulk density, is derived from the energy of the returning gamma rays. Porosity may also be derived from this bulk density, if the matrix density is known. In addition, the HLDS measures the photoelectric effect (absorption of low-energy gamma rays), which varies according to the chemical composition of the formation.

Borehole Compensated Sonic/Gamma

The borehole compensated sonic measures the traveltime of sound waves along the borehole wall between two transmitters and two receivers over distances 3 ft and 5 ft. The sonic velocity increases with compaction and lithification and will decrease in zones of higher porosity. An impedance log (density vs. velocity) can be used to generate synthetic seismograms for comparison with the seismic survey sections.

Operations

After coring operations ceased, the borehole was filled with freshwater gel mud, and the base of the drill pipe raised to ~33 mbsf. Each tool string was run sequentially in each hole, typically at logging speeds between 900 and 1800 ft/hr. After reaching the total depth of penetration, the tools were pulled upward at a constant rate to acquire the log data. The wireline heave compensator was used to minimize the effect of the ship's motion on the tool position.

Incoming data for each logging run were recorded and monitored in real time on the Schlumberger Maxis 500 logging computer. After logging, data were given preliminary interpretation. Schlumberger's GeoFrame software was used for processing the FMS images. The data were also transferred via high-speed data satellite link (Inmarsat B) to LDEO, where each logging run was shifted to a common depth scale and the NGT logs were recomputed. The processed data were then returned to the ship via the same satellite link and used in the site chapter report.

Vertical Seismic Profile

A two-ship vertical seismic profile (VSP) experiment was scheduled to be conducted by the Woods Hole Oceanographic Institution at Site 757 using their third-party three-component VSP tool. Because of the significant time shortage, the VSP experiment was canceled.

Data Quality

The principal influence on data quality is the state of the borehole wall. If the borehole width varies significantly over short intervals, or is more than 15 in wide, results from those tools (density, porosity, and FMS) that require good contact with the wall may be degraded. Very narrow sections will also cause irregular log results. The quality of the borehole is helped by minimizing the circulation of fluid during drilling and by logging a young hole.

Measurements that penetrate deeply into the formation, such as resistivity, are less sensitive to borehole conditions. Sonic velocity is more reliable in more compacted sediment or hard rocks. The maximum extent of the FMS pads is 15 in. Boreholes wider than this cannot be imaged adequately. Of the two natural-gamma tools, the HNGS has the more sensitive detector, and the data are corrected for borehole width in the tool itself; the NGT data requires shore-based reprocessing.

Log Depth Scales

The depth of the logged measurements is calculated from the length of cable minus the cable length to the seafloor (seafloor is identified by the step reduction in gamma-ray activity at the sediment/water boundary). Differences between the core depth and the log depth are due to factors such as core expansion, incomplete core recovery, and nonrecovery of the mudline. Drill-pipe depth, as measured by the logs, may be slightly different as a result of incomplete heave compensation, cable stretch (~1 m/km), and cable slip. There is also an effect from tides. All of these factors should be taken into account when using the logs.

SEISMIC MEASUREMENTS

Seismic While Drilling

Seismic while drilling (SWD; Rector et al., 1991) is a technique (Fig. F14) that uses an array of receivers on the seafloor to record seismic waves generated at the drill bit as drilling is under way. Its objective is similar to that of the more familiar VSP, in which a receiver is clamped at intervals down a borehole and a source fired at the sea surface. In an

F14. Geometry of the seismic while drilling experiment for Leg 179, p. 43.

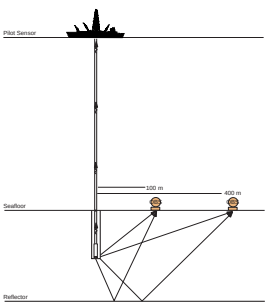

SWD-VSP experiment, the position of the source and receiver are reversed. Depending on the distribution of the receivers on the seafloor, wide-angle reflection information can also be obtained.

There are two significant advantages:

1. Measurements can be made without taking substantial rig time. Unlike a conventional VSP that uses borehole seismometers and generally takes 6–12 hr away from drilling time, a SWD-VSP expends ~1–2 hr for deployment and recovery of the seismometers. These can generally be accomplished during pipe trips requiring almost no additional ship time to accomplish the VSP. For this reason SWD-VSPs could allow seismic measurements to be made more frequently during future ODP legs.
2. With a suitable telemetry link and on-line processing, measurements can be made in near-real time, providing useful information to both drillers and scientists as the hole is being drilled.

Logistically, there are several factors that need to be addressed:

1. The seismic signal generated by the drill bit varies depending on bit type, weight on bit, rate of rotation, formation, and hole conditions.
2. Monitoring the output of the bit cannot be accomplished directly as with surface-fired sources. Source sensors are generally attached to the drill string well above the bit, in this case at the top of the drill string just below the top drive motor. The drill string is torsionally and longitudinally compliant and lengthens as stands of pipe are added.
3. Processing the data is considerably more complex, being based on long correlation sequences.
4. Although the shock induced by the bit as it penetrates the substrate is the major signal source, there are contributions to signal noise along the length of the drill string.
5. An array of receivers disposed on a flat seafloor cannot readily distinguish between the upward-moving sound generated by the drill bit and the downward-moving sound from the drilling ship. There is need to discriminate against the ship noise.

The experiment on this leg seeks to delimit the contributions of the various sound sources, how well the bit noise can be monitored from top of the drill string, the spectral distribution of the signals, and sources of noise.

The experimental set-up for this pilot experiment consists of one three-axis accelerometer (Summit Instruments, model 34103A) clamped on a short sub mounted directly below the 850-HP top-drive motor. The accelerometer's response is 1–80 Hz, dynamic range is 16 bits, and full scale is 5 g. The accelerometer signals are sampled 400 times per second. The data are telemetered from the rotating drill string to the lab using a FreeWave, model DGRO-115 902–928 MHZ spread spectrum radio. The module clamped on the sub is battery powered. Two ocean-bottom seismometer (OBS) systems, consisting of a three-axis seismometer (Mark Products, model L15B), a hydrophone, Onset Tattletale data recorder with an 800-MB disk, Benthos acoustic release, and battery pack are also included. These are housed in a 2-ft diameter aluminum sphere with an expendable 40-in diameter steel-plate anchor. One OBS is placed within 100 m of the hole, and the other

placed about four times the offset of the first seismometer. Additional OBSs would be useful, but only two were available for this feasibility study. The geophones (a velocity sensor) are gimbal mounted in a viscous oil bath. Their outputs are amplified 44 dB and 75 dB and bandpass filtered from 4.5 to 64 Hz. The signals are digitized with 12-bit resolution at two levels 30 dB apart, and the greater non-overdriven channel is recorded. Each channel is digitized at 200 samples per second. The locations of the OBSs with respect to the hole were determined by ranging on them while the drillship was maneuvering to spud in.

Leg 179 represented the first ocean drilling attempt to initiate and stabilize hard-rock holes on the seafloor with hammer bits before rotary coring. Thus, the leg provided the unique opportunity to record two quite different seismic sources, that of a hammer drill bit and the conventional rotary drill bit.

Offset Seismic Experiment

During Leg 179 an offset seismic experiment (OSE) was planned at Site 1107, the future Indian Ocean site in the International Ocean Network at the Ninetyeast Ridge. This experiment was designed as a two-ship experiment in collaboration with the German ship *Sonne,* which conducted a variety of seismic measurements at the Ninetyeast Ridge during its cruise SO 131 to determine the detailed crustal structure in that area (Flueh and Reichert, 1998). While the *Sonne* was acting as the shooting ship, a three-component borehole seismometer was to be deployed from the *JOIDES Resolution*. The receiver is a Geospace Wall-Lock Seismometer with a three-channel preamplifier, which can be remotely stepped through six gain settings in increments of 12 dB. Its sensing package consists of three sets of two 4.5-Hz geophones wired in series and aligned vertically and horizontally in two orthogonal directions. This instrument was used previously during Legs 102, 118, 123, 146, and 164. A detailed description of the tool can be found in the Leg 118 *Initial Reports* volume (Shipboard Scientific Party, 1989b). Two OBSs were deployed: one within 100 m of the drill hole; the other, within 500 m. In addition, 30 ocean-bottom hydrophones (OBHs, Flueh and Bialas, 1996) and OBSs, together with a newly constructed intraocean hydrophone, were deployed from the *Sonne*. Also, a three-channel ministreamer, with a total length of 200 m and an active length of 50 m, was used to record the air gun shots. Within a distance of 8 km from the borehole, the shot spacing was ~75 m; for greater distances, it was ~150 m. Because of the irregular distribution of anisotropy, the shots were made along several profiles with a nonequidistant distribution of azimuths and on circles with different radii. The planned layout of the OSE is shown in Figure **F15**.

The borehole seismometer would have complemented the OBH/OBS recordings. It has some advantages compared with a receiver at the ocean floor because of its position within the upper oceanic crust, the layer being studied (Swift et al., 1988). The borehole seismometer has (1) no direct water-wave arrival that obscures arrivals from shallow crust at short range, (2) a better signal-to-noise ratio because of the direct coupling to basement rocks, and (3) reduced uncertainty in the receiver location. Additionally, it is possible to determine the interval velocities in the vicinity of the borehole and to compare these velocities with results from other borehole and core measurements. Combined

F15. Planned radial and circumferential tracks of the shooting ship Sonne for the Leg 179 OSE, **p. 44.**

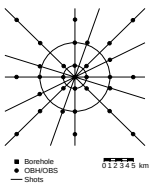

OBH/OBS and borehole seismometer recordings make it possible to determine a detailed velocity structure.

REFERENCES

Archie, G.E., 1942. The electrical resistivity log as an aid in determining some reservoir characteristics. *J. Pet. Technol.,* 5:1–8.

Blum, P., 1997. Physical properties handbook: a guide to the shipboard measurements of physical properties of deep-sea cores. *ODP Tech. Note,* 26.

Bouchez, J.L., Delas, C., Gleizes, G., Nedelec, A., and Cuney, M., 1992. Submagmatic microfractures in granites. *Geology,* 20:35–38.

Boyce, R.E., 1976. Definitions and laboratory techniques of compressional sound velocity parameters and wet-water content, wet-bulk density, and porosity parameters by gravimetric and gamma-ray attenuation techniques. *In* Schlanger, S.O., Jackson, E.D., et al., *Init. Repts. DSDP,* 33: Washington (U.S. Govt. Printing Office), 931–958.

Cannat, M., Karson, J.A., and Miller, D.J., et al., 1995. *Proc. ODP, Int. Repts.,* 153: College Station, TX (Ocean Drilling Program).

Dick, H.J.B, Natland, J., Miller, D.J., et al., 1999. *Proc. ODP, Init. Repts.,* 176: College Station, TX (Ocean Drilling Program).

Ellis, D.V., 1987. *Well Logging for Earth Scientists:* New York (Elsevier).

Flueh, E.R., and Bialas, J., 1996. A digital, high data capacity ocean bottom recorder for seismic investigations. *Int. Underwat. Syst. Des.,*18:18–20.

Flueh, E.R., and Reichert, C., 1998. Cruise Report SO 131 SINUS. *GEOMAR Rept.,* 72:1–337.

Hirth, G., and Kohlstedt, D.L., 1995. Experimental constraints on the dynamics of the partially molten upper mantle: deformation in the diffusion creep regime: *J. Geophys. Res.,* 100:1981–2001.

Irvine, T.N., 1982. Terminology for layered intrusions. *J. Petrol.,* 23:127–162.

Le Maitre, R.W., 1989. *A Classification of Igneous Rocks and Glossary of Terms:* Oxford (IUGS, Blackwell).

Means, W.D., and Park, Y., 1994. New experimental approach to understanding igneous texture. *Geology,* 22:323–326.

Nicolas, A., and Ildefonse, B., 1996. Flow mechanisms and viscosity in basaltic magma chambers. *Geophys. Res. Lett.,* 23:2013–2016.

Rector, J.W., III, and Marion, B.P., 1991. The use of drill-bit energy as a downhole seismic source. *Geophysics,* 56:628–634.

Rider, M., 1996. *The Geological Interpretation of Well Logs:* Caithness (Whittles Publishing).

Serra, O., 1984. *Fundamentals of Well-Log Interpretation* (Vol. 1): *The Acquisition of Logging Data.* Dev. Pet. Sci., 15A: Amsterdam (Elsevier).

Serra, O., 1986. *Fundamentals of Well-Log Interpretation* (Vol. 2): *The Interpretation of Logging Data.* Dev. Pet. Sci., 15B: Amsterdam (Elsevier).

Serra, O., 1989. *Formation Microscanner Image Interpretation:* Houston (Schlumberger Educ. Services), SMP-7028.

Shipboard Scientific Party, 1989a. Introduction and Explanatory Notes. *In* Robinson, P.T., Von Herzen, R., et al., *Proc. ODP, Init. Repts.,* 118: College Station, TX (Ocean Drilling Program), 3–23.

Shipboard Scientific Party, 1989b. Site 735. *In* Robinson, P.T., Von Herzen, R., et al., *Proc. ODP, Init. Repts.,*118: College Station, TX (Ocean Drilling Program), 89–222.

Shipboard Scientific Party, 1991. Explanatory Notes. *In* Taira, A., Hill, I., Firth, J.V., et al., *Proc. ODP, Init. Repts.,* 131: College Station, TX (Ocean Drilling Program), 25–60.

Shipboard Scientific Party, 1992a. Explanatory Notes. *In* Parson, L., Hawkins, J., Allan, J., et al., *Proc. ODP, Init. Repts.,* 135: College Station, TX (Ocean Drilling Program), 49–79.

Shipboard Scientific Party, 1992b. Explanatory Notes. *In* Dick, H.J.B., Erzinger, J., Stokking, L.B., et al., *Proc. ODP, Init. Repts.,* 140: College Station, TX (Ocean Drilling Program), 5–33.

Shipboard Scientific Party, 1992c. Explanatory Notes. *In* Behrmann, J.H., Lewis, S.D., Musgrave, R.J., et al., *Proc. ODP, Init. Repts.,* 141: College Station, TX (Ocean Drilling Program), 37–71.

Shipboard Scientific Party, 1993a. Explanatory Notes. *In* Gillis, K., Mével, C., Allan, J., et al., *Proc. ODP, Init. Repts.,* 147: College Station, TX (Ocean Drilling Program), 15–42.

Shipboard Scientific Party, 1993b. Explanatory Notes. *In* Alt, J.C., Kinoshita, H., Stokking, L.B., et al., *Proc. ODP, Init. Repts.,* 148: College Station, TX (Ocean Drilling Program), 5–24.

Shipboard Scientific Party, 1995. Explanatory Notes. *In* Cannat, M., Karson, J.A., Miller, D.J., et al., *Proc. ODP, Init. Repts.,* 153: College Station, TX (Ocean Drilling Program), 15–42.

Shipboard Scientific Party, 1999. Explanatory Notes. *In* Dick, H.J.B, Natland, J., Miller, D.J., et al., *Proc. ODP. Init. Repts.,* 176: College Station, TX, (Ocean Drilling Program), 1–42.

Swift, S.A., Stephen, R.A., Hoskins, H., 1988. Structure of upper oceanic crust from an oblique seismic experiment at Hole 418A, Western North Atlantic. *In* Salisbury, M.H., Scott, J.H., et al., *Proc. ODP, Sci. Results,* 102: College Station, TX (Ocean Drilling Program), 97–124.

Timur, A., and Toksöz, M.N., 1985. Downhole geophysical logging. *Annu. Rev. Earth Planet. Sci.,* 13:315–344.

Twiss, R.J., and Moores, E.M., 1992, *Structural Geology:* New York (Freeman), 53.

Wager, L.R., Brown, G.M., and Wadsworth, W.J., 1960. Types of igneous cumulates. *J. Petrol.,* 1:73–85.

Williams, H., Turner, F. J., and Gilbert, C. M., 1982. *Petrography: An Introduction to the Study of Rocks in Thin Sections* (2nd ed.): New York (Freeman).

Figure F1. Diagram illustrating terms used in the discussion of coring operations and core recovery.

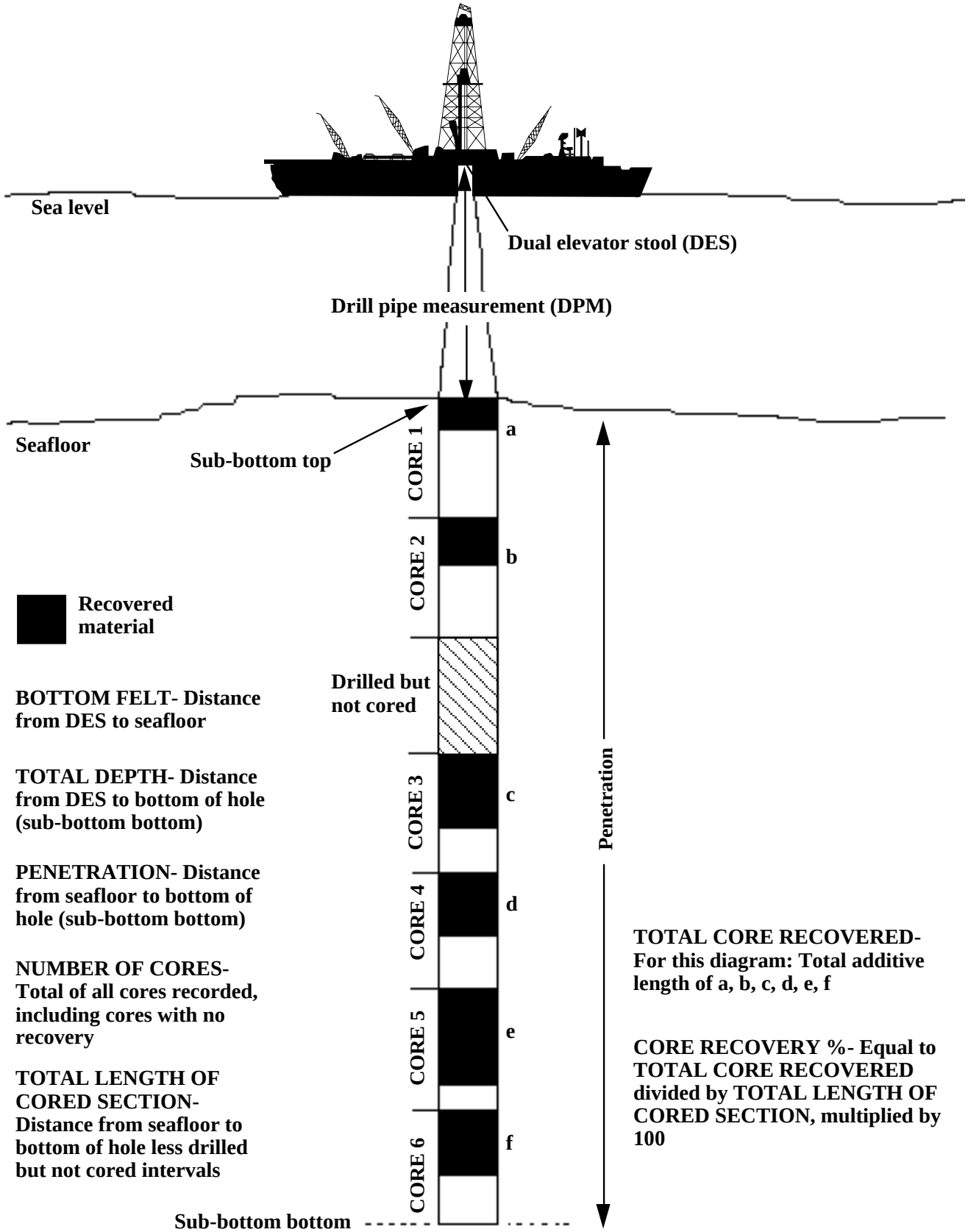

Figure F2. Diagram illustrating hard-rock core division procedures.

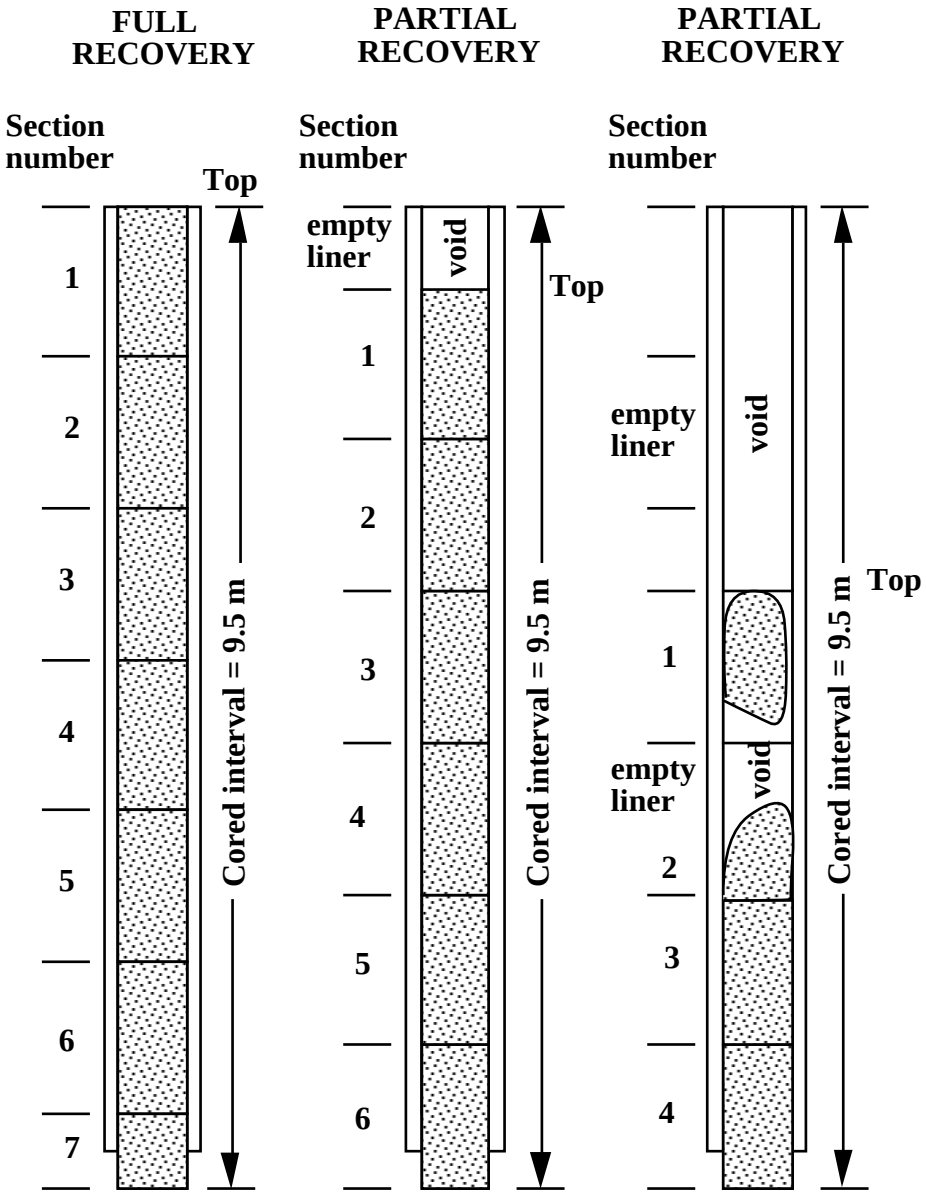

Figure F3. This figure illustrates core curation procedures for hard rocks. Letters designating pieces as removed from core barrel are for illustrative purposes only. Pieces A, B, C, D, E, and F become interval XXX-YYYZ-1R-01, Piece 1 to Piece 6 (where XXX is the leg, YYY is the site, and Z is the hole designator, respectively). Since pieces G and H can be reoriented to fit along a fracture, they are curated as a single piece. In this case, the reassembled single piece is too long to fit in the bottom of Section 1R-01, so it is shunted to the top of Section 1R-02 and curated as interval XXX-YYYZ-1R-02, (Pieces 1A and 1B). Similarly, pieces L and M are too long to fit in the bottom of Section 1R-02 after realignment and are shunted to the top of Section 1R-03. Spacers between pieces also artificially add length to the core when measured for archiving and curation. For example, pieces L and M represent an interval from 2.17 to 2.63 m down from the top of the core as removed from the core barrel but are archived as interval XXX-YYYZ-1R-03 (Pieces 1A and 1B, 0.0–46.0 cm).

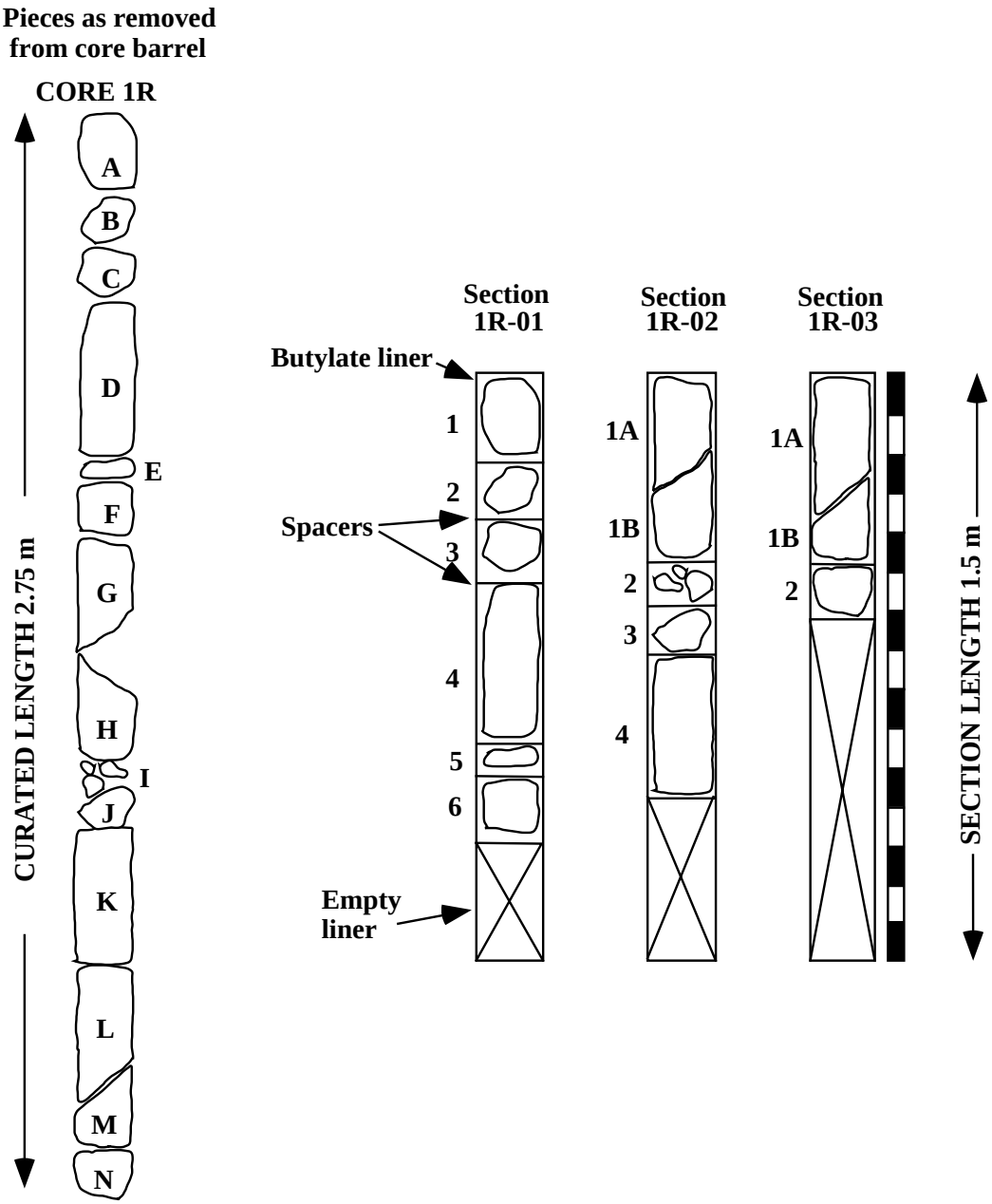

Figure F4. Example of gabbro hard-rock visual core description (HRVCD) form.

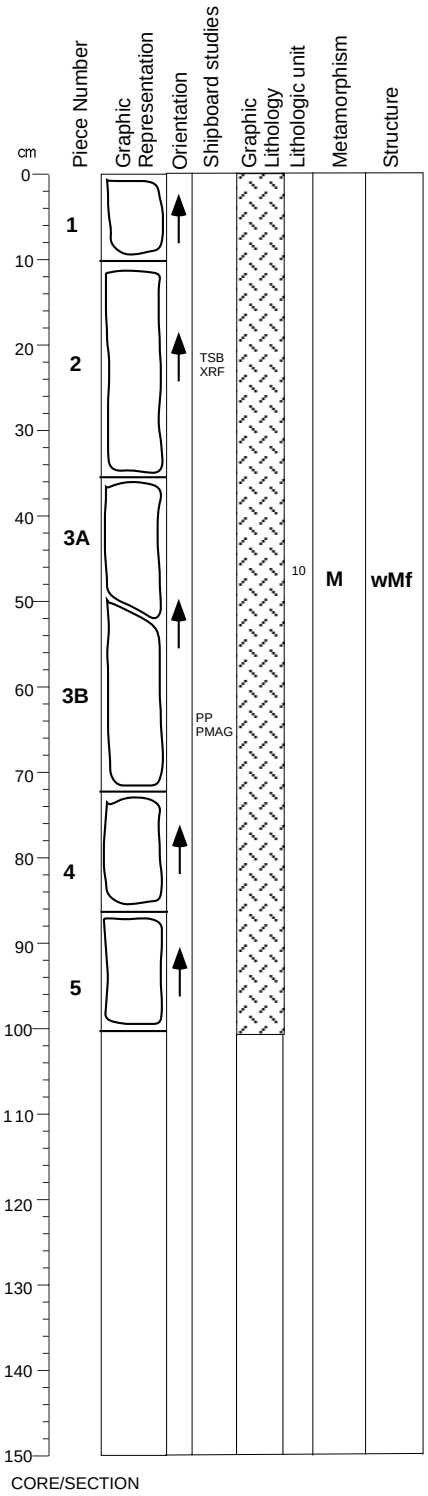

179-1104B-8R-1

UNIT: 10 **GABBRO**

Interval Location:	**Core**	**Section**	**Piece**	**Depth in Section**	**Depth mbsf**
Upper contact:	**8R**	**1**	**1**	**0**	**55.0**
Lower contact:	**8R**	**1**	**5**	**100**	**56.0**
Thickness (m):	**1**				
Contact Type:	**missing**				

	%	**Grain Size (mm):**			
	Mode	**Max**	**Min**	**Avg. Size**	**Shape/Habit**
Plagioclase	60	10	3	coarse	tabular/anhedral
Clinopyroxene	35	100	2	coarse	equant/oikocrystic
Olivine	4.5	25	3	coarse	ameoboidal/anhedral
Opaques	0.5				
Total	**100**				

GRAIN SIZE: Coarse

TEXTURE: Intergranular

STRUCTURE: No plastic deformation. Weak magmatic fabric.

ALTERATION: Low to moderate background alteration (as high as 20%). Rare amhibole veins, and some amphibole rimming clinopyroxene.

COMMENTS: Olivine is variably altered near fractures. Clinopyroxene mode is variable. Some of the clinopyroxene is pegmatitic.

Figure F5. Graphic lithology patterns used during Leg 179.


Gabbro


Olivine gabbro


Oxide gabbro


Oxide olivine gabbro


Oxide olivine microgabbro


Aplitic/felsic vein

Figure F6. A. Classification of ultramafic and gabbroic rocks composed of olivine, clinopyroxene, orthopyroxene, and plagioclase (after Le Maitre, 1989). (Continued on next two pages.)

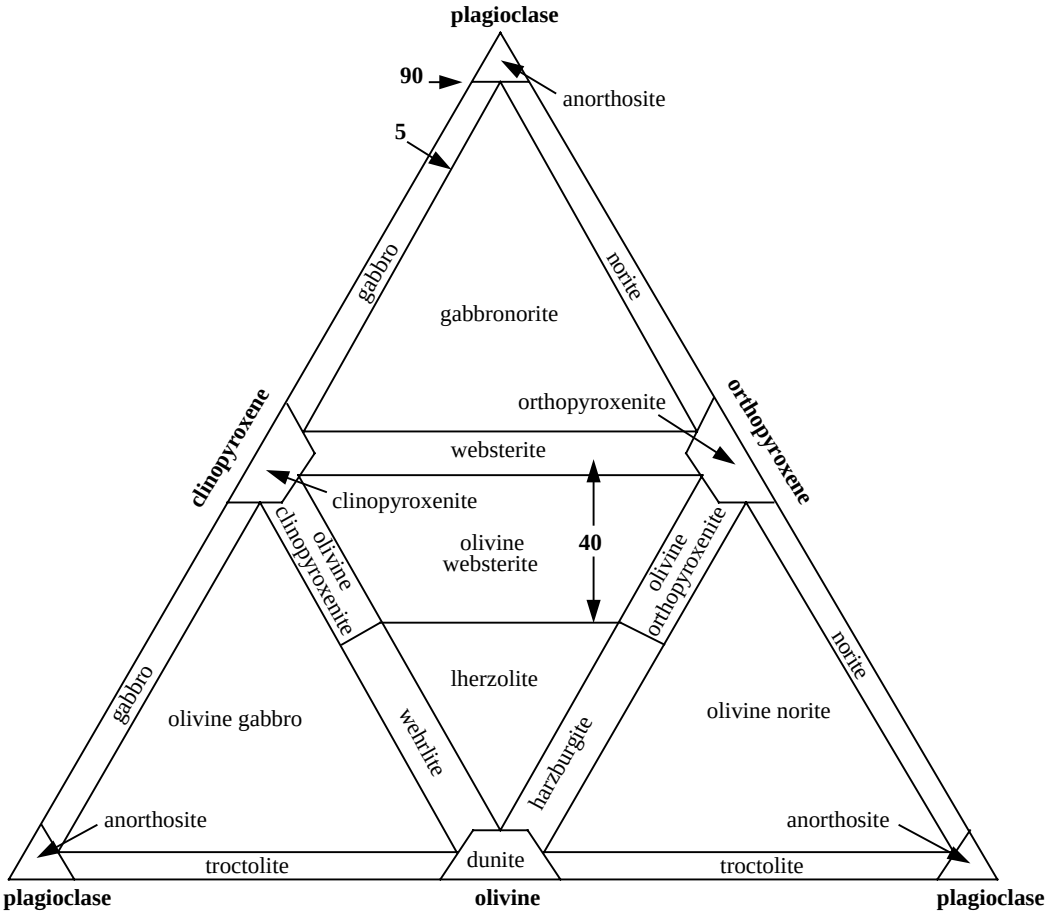

Figure F6 (continued). B. Classification of gabbroic rocks composed of plagioclase, hornblende, and pyroxene (after Le Maitre, 1989).

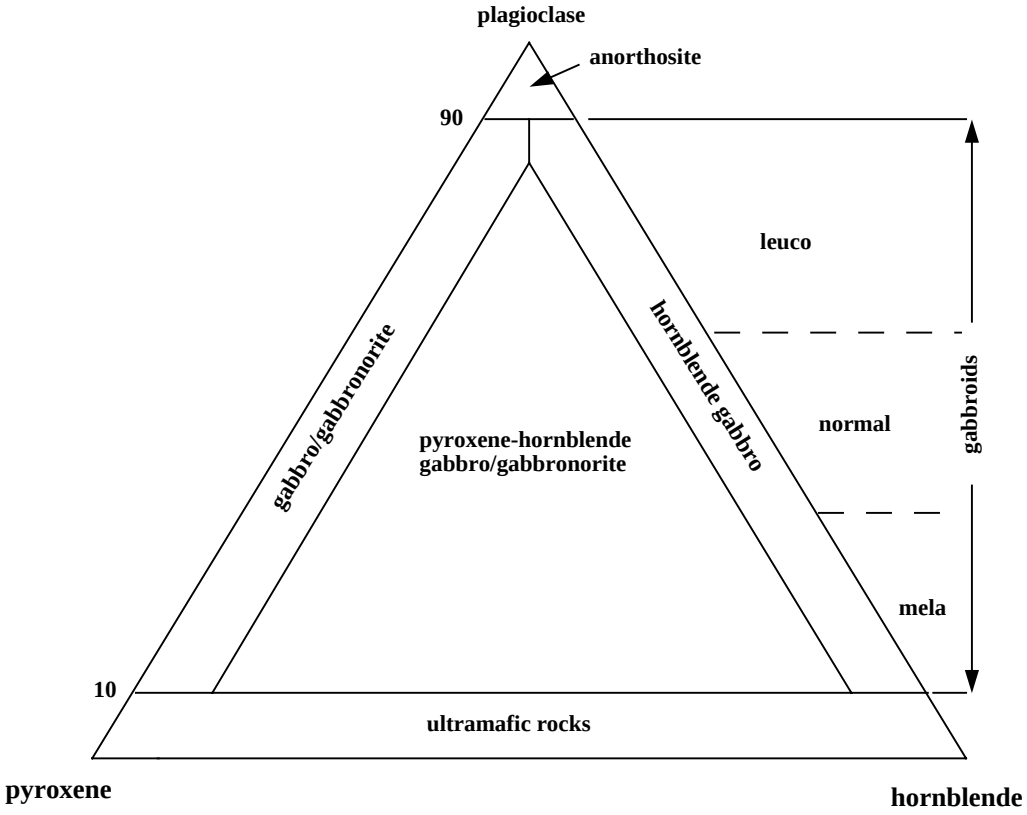

Figure F6 (continued). C. Classification of silicic plutonic rocks composed of quartz, plagioclase, and alkali feldspar (after Le Maitre, 1989).

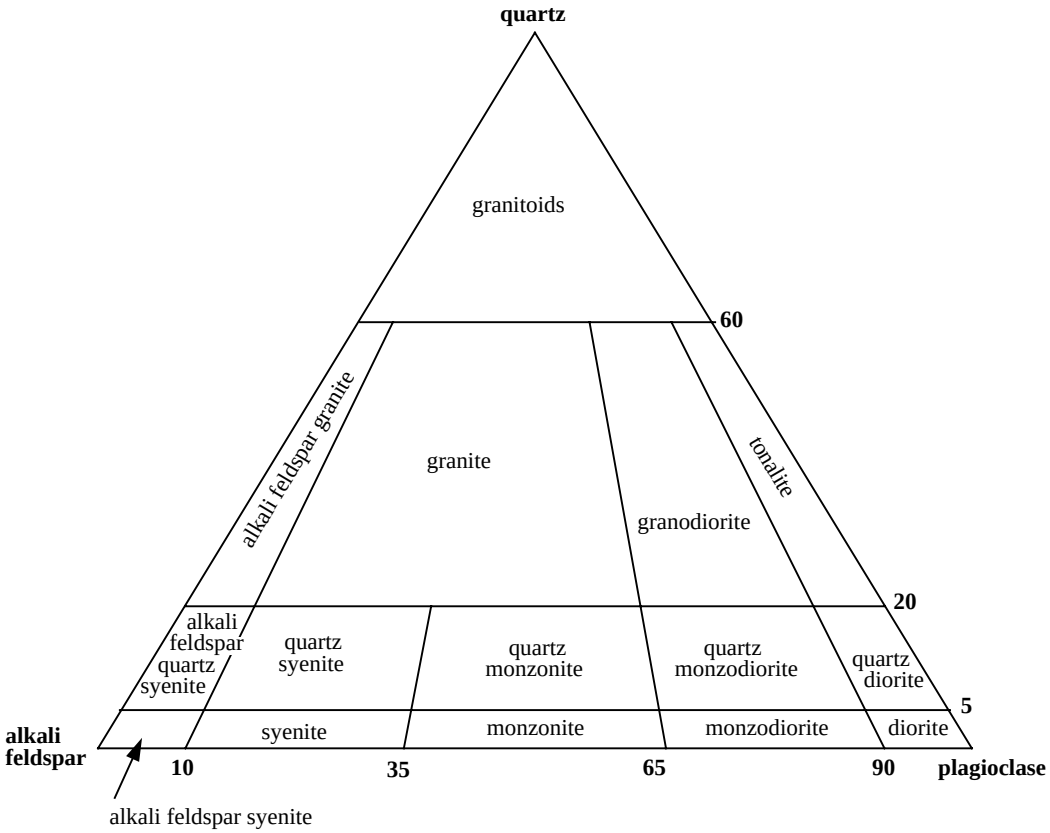

Figure F7. Example of the spreadsheets used during Leg 179 for igneous/metamorphic core description. (Continued on next five pages.)

Leg 179 Igneous/metamorphic core log														
		Lower contact									**Rock type**			
Lithol.				Depth		Depth	Interval				Grain	Modifier	Rock	Special
Interv.	Leg-Hole	Core	Sec.	cur.	Pc.	mbsf	Thickn.	Type	Form		Size		Name	Modifier

Figure F7 (continued).

Leg 179 Mineralogy log: mode and grain-size					Mineralogy																			
					Plagioclase					Clinopyroxene					Olivine					Opx/Pig				
Interval	Leg-Hole	Core	Sect.	Piece	%	Max	Min	Avg	Alt%	%	Max	Min	Avg	Alt%	%	Max	Min	Avg	Alt%	%	Max	Min	Avg	Alt%

Figure F7 (continued).

Leg 179 Mineralogy log: mode													
and grain-size (con't)													
					Opaques	**Sulfides**	**Unidentified**		**Grain size**	**Difference**		Total	
Interval	Leg-Hole	Core	Sect.	Piece	%	%	%	**Total**	**weighted avg.**	**from 100**		Alteration%	

Figure F7 (continued).

Leg 179 Textures							equant, tabular, platy, elongate, accicular, amoeboidal, angular, globular,			
					Mineral shape		interstitial			
Interval	Leg-Hole	Core	Sect.	Piece	plagioclase	clinopyroxene	olivine	orthopyroxene	opaques	sulfides

Figure F7 (continued).

Leg 179 Textures					euhedral, subhedral, anhedral, chadacrystic, oikocrystic, rounded, deformed, fractured, disseminated, matrix,					
(con't)			**Mineral habit**		concordant seams, discordant seams, disseminated in oxides, disseminated in silicates, massive, interstitial					
Interval	Leg-Hole	Core	Sect.	Piece	plagioclase	clinopyroxene	olivine	opx./pig.	opaques	sulfides

Figure F7 (continued).

Leg 179 Textures					igneous lamination, schlieren, clusters, subophitic				
(con't)					ophitic, poikilitic, equigranular, intergranular				
					Fabrics			**MM Facies**	**Comments**
Interval	Leg-Hole	Core	Sect.	Piece	**type**	**dist** (uniform, variable)			

Figure F8. An example of the structural log spreadsheet devised for computer storage and manipulation of structural data derived from the core description.

LOG					FEATURE			POSITION			VEINS AND DIKES					PLANAR				LINEAR	CORR. ORIENT		FAULTS and SHEAR ZONES					Comments
Hole	Core	Section	Piece	Oriented?	Identifier	Texture	Intensity	Top	Bottom	mbsf to top of struct.	Min/Compos.	Est. % area	Array Density (#/m)	Width (mm)	Length (mm)	Apparent dip + dir	Apparent dip + dir2	Strike	Dip	Plunge & Trend	Strike & Dip	Plunge & Trend	Nature of Fault-Rock	App. Shear Sense	Zone Thickness	Displacement (mm)	Cross-Cutting Rel.	

Figure F9. Key to structural identifiers used during Leg 179. See text for discussion.

	Leg 179 Structural Identifiers	
Identifiers	Planar Feature	Linear Feature
J	Joints	
SHM	Drilling Induced Sub-horizontal Microcracks	
AV	Alteration Veins	Mineral Growth Direction
MV	Magmatic Veins	Mineral Growth Direction
DC	Igneous Dike Contact	Mineral Lineation
IPC	Igneous Pluton Contact	
F	Faults	Slickenlines
B	Fault Breccias	Slickenlines
MB	Magmatic Breccias	
CB	Cataclastic Breccias	
BFZ	Brittle Fault Zone	Slickenlines
CSZ	Cataclastic Shear Zone	
MSZ	Mylonitic Shear Zone	Mineral Lineation
DSZ	Ductile Gneissic Shear Zone	Mineral Lineation
AF	Anastomosing Foliation	Mineral Lineation
DF	Disjunctive Foliations	Mineral Lineation
CPF	Crystal-Plastic Shape Fabric	Mineral Lineation
FO	Folds	Fold Hinge
MF	Magmatic Fabric	Mineral Lineatiom
ILC	Igneous Layer Contact	
ILZ	Zone of Fine Scale Igneous Layering	
TI	Boundary Between Tectonite and Igneous Textured Rock	
B	Bedding	
UNC	Unconformities	
VFB	Volcanic Flow Boundaries	

Figure F10. Table showing checklist used for spreadsheet comments associated with each structural identifier.

STRUCTURAL IDENTIFIERS AND COMMENTS CHECKLIST
LEG 179
STRUCTURAL GEOLOGY

The following is a checklist of structural characteristics (modified from Cannat, Karson, Miller et al., 1995) that were searched for in macroscopic core samples. These characteristics supplement the information required by the spreadsheet and were noted in the comments section of the Structural Log spreadsheet (Fig. F8) and Structural Notebook.

The feature-identifier code and a number corresponding to the *n*th feature in the each piece of the core are entered in the Identifier column of the spreadsheet and in the comments column if needed (i.e.,V3). The feature identifier is cross-referenced to the sketch in the visual core description.

Subhorizontal Microcracks (SHM)
- Drilling induced fractures.

Joints (J)
- Joint density;
- Orientation; and
- Plume structures on joint surface.

Alteration Veins (AV) / Magmatic Veins (MV)
- Orientation of veins and vein-array boundaries;
- Magnitude and nature of offset;
- Density of vein network;
- Array characteristics:
  - ~ Sense of shear,
  - ~ Angle between new vein segments and array boundary (measure of array dilatation);
- Internal structure of fibers;
- Crack-seal structures and number of vein-opening events;
- Wall-rock alteration and shape;
- Vein terminations (splayed or tapered); and
- Vein mineralogy.

Faults (F) and Fault Zones (FZ)
- Fault-zone thickness, orientation and density;
- Movement sense (r,n,d,s), reverse, normal, dextral sinistral;
- Slickenlines;
- Matrix material (gouge or secondary minerals);
- Overprinting of pre-existing fabric; and
- Semi-brittle.

Semi-Brittle and Ductile Shear Zones: Cataclastic (CSZ), Mylonitic (MSZ), Ductile Gneissic (DSZ).
- Intensity of cataclastic, mylonitic or crystal plastic fabric;
- Movement sense (r,n,d,s), reverse, normal, dextral sinistral; and
- Change in orientation of foliation and direction of intersection of shear zone margin and foliations.

Breccias: Fault Breccias (FB)
Magmatic Breccias (MB), Cataclastic Breccia (CB)
- Clast size and shape, matrix composition, relative proportions.

Foliations: Anastomosing (AF), Disjunctive (DF)
- Style of foliation (e.g., crenulation (Cc), spaced (Cs));
- Spacing or wavelength; and
- Angle between folaition and earlier fabrics, noting directions of larger-scale fold closures.

Crystal-Plastic Fabrics (CPF)
- Intensity of fabric;
- Intensity of retrograde fabric (PrR);
- Orientation of foliation (Sp) and lineation (Lp);
- L-, LS- and S-tectonite; and
- Shear sense indicators: block-rotated porphyroclasts, asymmetric augen, SC fabrics, discrete shear bands, mica, fish, and tension-gash arrays; (r,n,d,s), reverse, normal, dextral sinistral;- mineralogical segregation or banding.

Folds (FO)
- Inter-limb angle;
- Estimate of hinge curvature (e.g., kink vs. round);
- Asymmetry of hingeline relative to other fabrics (e.g., stretching lineations, etc.);
- Other geometrical aspects preserved in core (e.g., wavelength, amplitude, etc.); and
- Number of folds, if more than one.

Magmatic Fabrics (MF)
- Intensity and orientation of foliations (Sm) and lineations (Lm);
- Minerals that define the shape and/or crystallographic preferred orientations;
- Angle between crystallographic and shape fabrics; and
- Orientation of subfabrics.

Compositional Layering (Cl)/Gradational Boundaries (Gb)
- Type of layering (e.g., sedimentary, igneous cumulate, alteration etc.);
- Orientation, thickness and density of layers.

Igneous Contacts: Dike Contact (DC)
Non-Tabular Pluton Conatct (PC)
- Orientation and density; and
- Concordant or discordant.

Igneous Layer Contact (ILC)
Zone of Fine-Scale Igneous Layering (ILZ)
- Type of layering;
- Orientation;
- Contact type;
- Scale and thickness of layers; and
- Sharp or gradational.

Cross-Cutting Relationships
- Intrusive relationships, relative chronology of the different fabrics; and
- Angle between compositional layering and magmatic or crystal-plastic fabric.

Boundary Between Tectonites and Igneous Textured Rock (TI)
- Nature of contact.

Volcanic Flow Boundary (VFB)
- Upper or lower;
- Extent of chilled margin;
- Regularity; and
- Orientation.

Unconformity (UNC)
- Relief;
- Weathering zone thickness; and
- Orientation.

Bedding (B)
- Orientation.

Figure F11. Table showing intensity scales applied to structural identifiers for brittle and ductile deformation (from Shipboard Scientific Party, 1995). The intensity of joints and faults is related to spacing estimated by the linear intercept method along the central divide of the core piece. If a piece was unoriented, then spacing was estimated along the long axis of the piece. Vein intensity is related to an estimation of percentage of veining on the cut face of the archive half of the core. This scale has been subdivided into seven groups so that the relatively low percentages encountered during Leg 153 could be distinguished. Brecciation intensity relates to the relative percentage of clasts to matrix. Foliations and crystal-plastic fabrics broadly relate to the attenuation of porphyroclasts and/or the spacing of foliation planes. Fold intensity relates to the interlimb angle for individual or multiple folds. Layering intensity relates only to the layer width and was applied to any layers with discrete or gradational boundaries. Such layers included primary magmatic layering, alteration, or grain-size variations. Magmatic deformation intensity relates broadly to the degree of shape preferred orientation of magmatic phases.

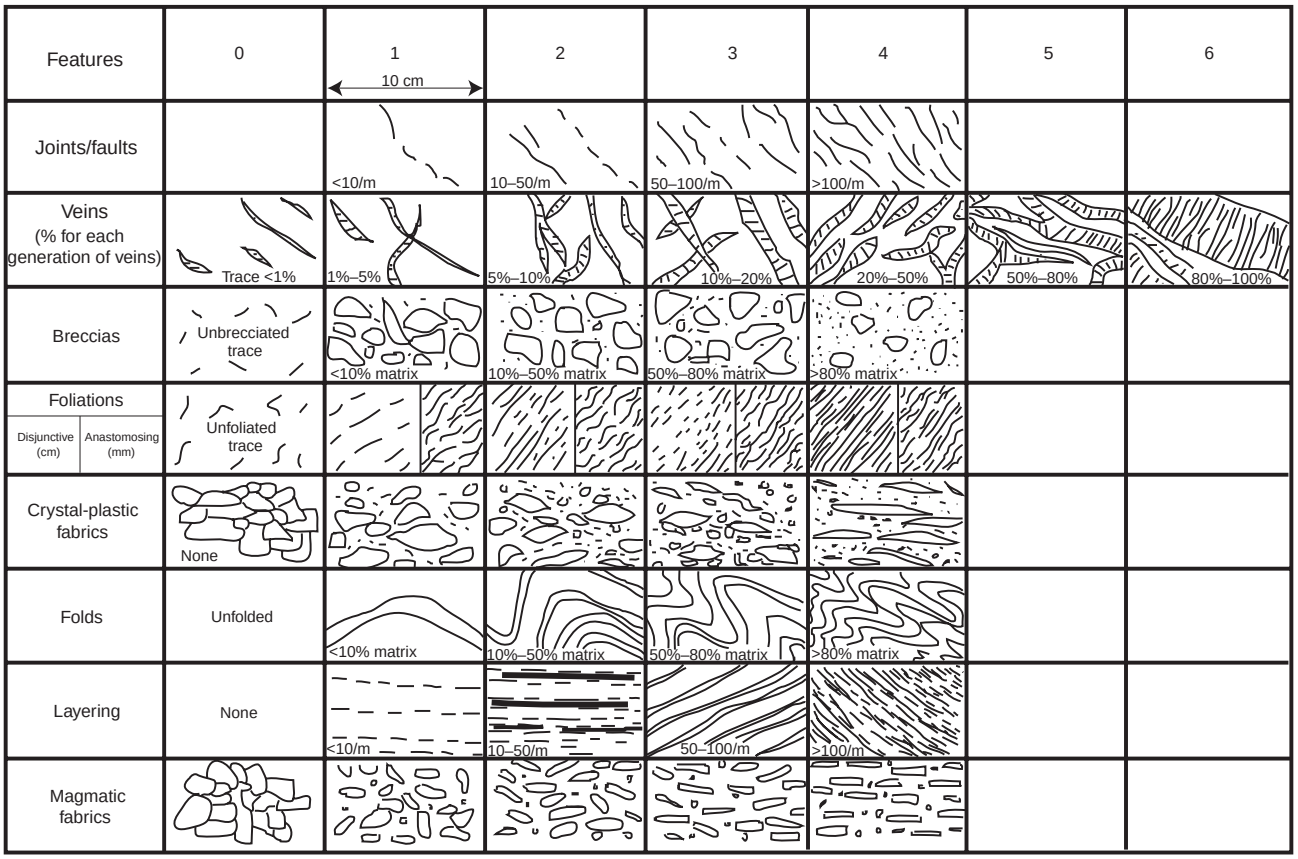

Figure F12. Key to textural features entered in structural VCDs and summary spreadsheet.

Textures	Code	Abreviation
Protogranular	1	PG
CG Equigranular	2	CGE
Porphyroclastic	3	PC
Elongate Porphyroclastic	4	EPC
Mylonitic	5	MYL
UltraMylonitic	6	UMYL
Cataclastic	7	CAT
Equigranular Gneiss	8	EG
Augen Gneiss	9	AG
Schistose	10	SCH

Figure F13. Downhole logging tool strings used for Leg 179.

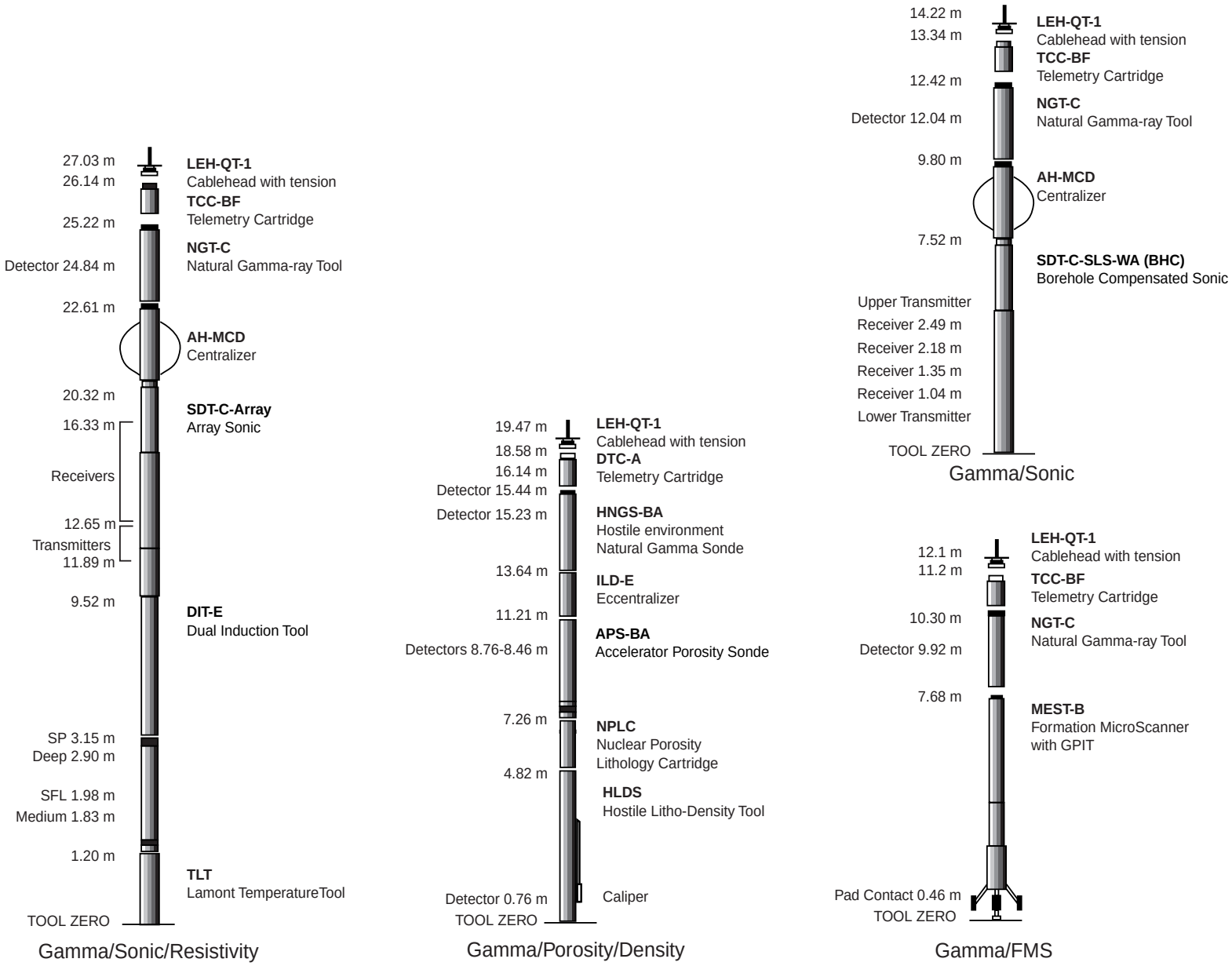

Figure F14. Geometry of the seismic while drilling experiment for Leg 179.

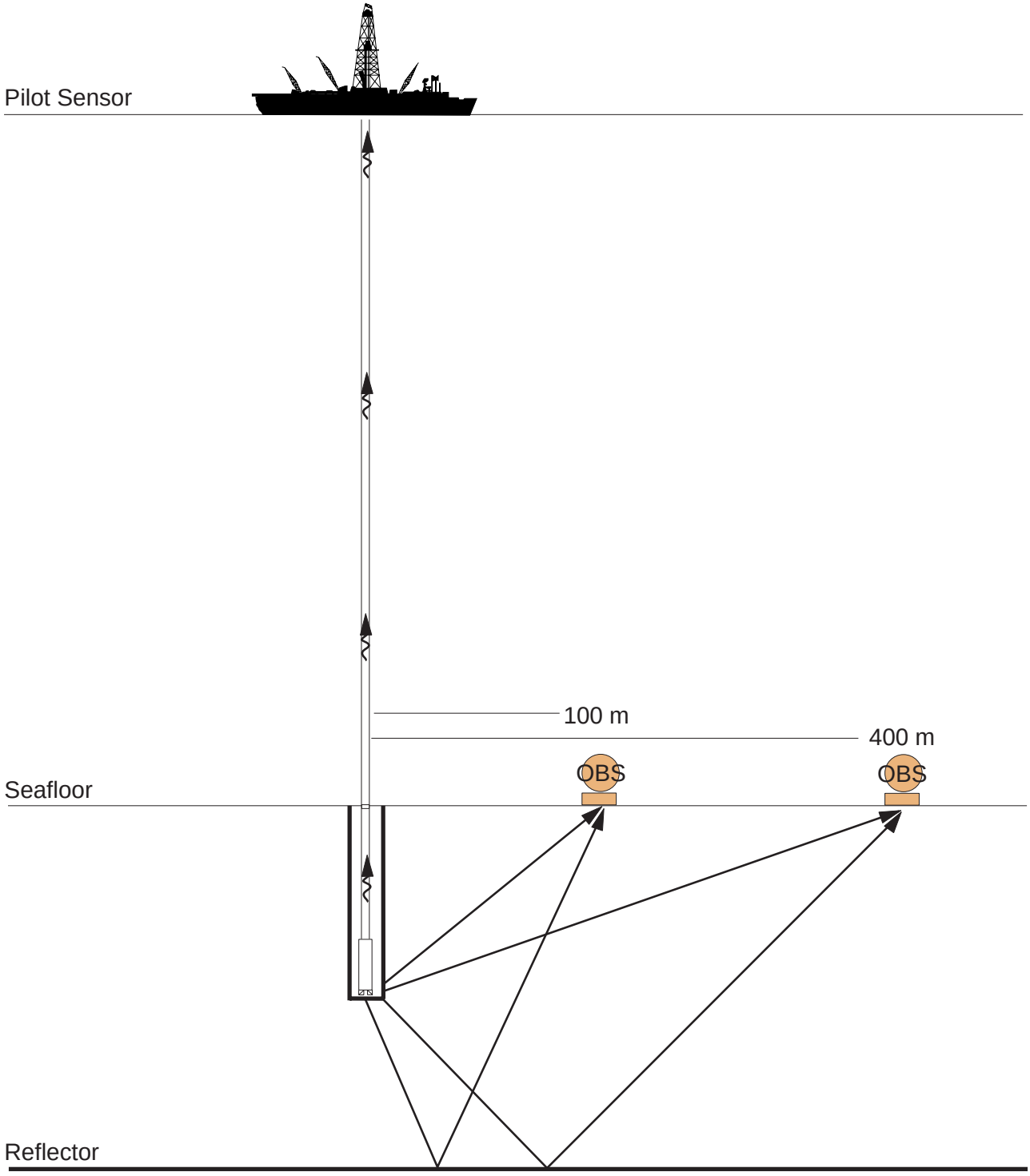

Figure F15. Planned radial and circumferential tracks of the shooting ship *Sonne* for the Leg 179 OSE.

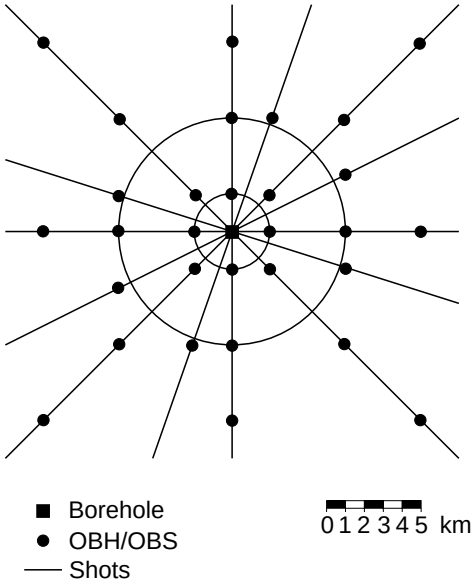

Table T1. XRF analytical conditions for Leg 179.

Oxide or element	Line	Crystal	Detector	Collimator	Peak angle (°2θ)	Background offset (°2θ)	Count time on peak (s)	Count time on background (s)	Analytical error (rel %)	Detection limit
SiO_2	Kα	PET	FPC	Medium	109.21		40		0.30	0.03
TiO_2	Kα	LIF200	FPC	Fine	86.14		40		0.37	0.01
Al_2O_3	Kα	PET	FPC	Medium	145.12		100		0.40	0.01
Fe_2O_3	Kα	LIF200	FPC	Fine	57.52		40		0.20	0.01
MnO	Kα	LIF200	FPC	Fine	62.97		100		0.10	0.005
MgO	Kα	TLAP	FPC	Medium	45.17	±0.80	150	150	0.60	0.01
CaO	Kα	LIF200	FPC	Medium	113.09		40		0.30	0.005
Na_2O	Kα	TLAP	FPC	Medium	54.10	–1.20	150	150	3.8	0.03
K_2O	Kα	LIF200	FPC	Medium	136.69		100		0.40	0.01
P_2O_5	Kα	GE111	FPC	Medium	141.04		100		0.40	0.01
Rh	Kα Compton	LIF200	Scint	Fine	18.58		60			
Nb	Kα	LIF200	Scint	Fine	21.40	+0.35	200	100	0.2	0.5
Zr	Kα	LIF200	Scint	Fine	22.55	–0.35	100	50	0.5	0.6
Y	Kα	LIF200	Scint	Fine	23.80	–0.40	100	50	1.0	0.6
Sr	Kα	LIF200	Scint	Fine	25.15	–0.40	100	50	0.3	0.6
Rb	Kα	LIF200	Scint	Fine	26.62	–0.60	100	50	3.6	0.6
Zn	Kα	LIF200	Scint	Medium	41.81	–0.55	100	50	1.0	1.0
Cu	Kα	LIF200	Scint	Fine	45.03	–0.55	100	50	1.5	1.2
Ni	Kα	LIF200	Scint	Medium	48.67	–0.60	100	50	0.6	1.2
Cr	Kα	LIF200	FPC	Fine	69.35	–0.50	100	50	1.3	2.0
V	Kα	LIF220	FPC	Fine	123.06	–0.50	100	50	2.0	3.0
Ti	Kα	LIF200	FPC	Fine	86.14	+0.50	40	20		
Ce	Lα	LIF220	FPC	Medium	128.13	–1.50	100	50		
Ba	Lß	LIF220	FPC	Medium	128.78	–1.50	100	50		

Notes: All major elements measured using a Rhodium X-ray tube operated at 30 kV and 80 mA. Trace elements are measured using a Rhodium X-ray tube operated at 60 kV and 50 mA. Detector: FPC = flow proportional counter (P10 gas); Scint = NaI Scintillation counter. Detection limit units = weight percent for major elements, parts per million for trace elements.

Table T2. Schlumberger tool and measurement acronyms.

Tool	Output	Explanation	Units
HNGS		Hostile environment natural gamma sonde	
	HSGR	Standard (total) gamma ray	gAPI
	HCGR	Computed gamma ray (HSGR minus uranium contribution)	gAPI
	HFK	Formation potassium	Percent million
	HTHO	Thorium	Parts per million
	HURA	Uranium	Parts per million
NGT		Natural gamma tool	
	SGR	Standard (total) gamma ray	gAPI
	CGR	Computed gamma ray (SGR minus uranium contribution)	gAPI
	POTA	Potassium	Percent million
	THOR	Thorium	Parts per million
	URAN	Uranium	Parts per million
APS		Accelerator porosity sonde	
	APLC	Near/array porosity (limestone corrected)	Fraction
	FPLC	Near/far porosity (limestone corrected)	Fraction
	SIGF	Neutron capture cross section of the formation	Capture units
	STOF	Tool standoff (computed distance from borehole wall)	Inches
HLDS		High temperature litho-density sonde	
	RHOM	Bulk density (corrected)	Grams per cubic centimeter
	PEFL	Photoelectric effect	Barns per electron
	LCAL	Caliper - measure of borehole diameter	Inches
	DRHO	Bulk density correction	Grams per cubic centimeter
DIT		Dual induction tool	
	IDPH	Deep induction phasor-processed resistivity	Ohm-meter
	IMPH	Medium induction phasor-processed resistivity	Ohm-meter
	SFLU	Spherically focused resistivity	Ohm-meter
SDT		Digital sonic tool	
	LTT1-4	Transit times (10-, 8-, 12-, 10-ft transmitter-receiver spacings)	Microsecond
	DTLF	Slowness (12 minus 10 ft traveltimes)	Microsecond per foot
	DTLN	Slowness (10 minus 8 ft traveltimes)	Microsecond per foot
BHC		Borehole compensated sonic tool	
	LTT1-4	Transit times	Microsecond
	DT	Slowness	Microsecond per foot

Table T3. Specifications of the downhole tools deployed during Leg 179.

Tool string	Tool	Measurement	Sample interval (cm)	Approximate vertical resolution (cm)
Resistivity/Sonic	SDT	Sonic velocity	15	120
	DIT*	Resistivity	2.5 and 15	200/150/75
	NGT*	Natural gamma	15	45
	TLT	Borehole fluid temperature	1/s	—
FMS-sonic (total length ~12 m)	NGT*	Natural gamma	15	45
	GPIT*	Tool orientation	15	—
	FMS*	Resistivity image	0.25	0.5
Porosity/Density (total length ~19.5 m)	HNGS*	Natural gamma	15	45
	APS*	Porosity	5 and 15	30
	HLDS*	Bulk density, PEF	2.5 and 15	15/45
BHC (total length ~14 m)	NGT*	Natural gamma	15	45
	BHC*	Borehole compensated sonic	15	61

Notes: * = trademarks of Schlumberger. See Table T2 for explanations of the acronyms.